This article presents a nice and detailed investigation of the photolysis, ozonolysis and OH-reaction of a conjugated carbonyl nitrate produced in the oxidation of isoprene by NO3 radical. The topic is of great importance to atmospheric chemistry since the formation and fate of organic nitrates play an outstanding role through their influence on the budget of NOx over forested areas. The methods are appropriate and the analysis is sound (with some minor reservations as explained further below). The article is also very well-written, very clear, and appropriately illustrated. Although the focus is on a specific compound which in itself plays probably only a very minor role in the atmosphere, the results regarding the rates of photolysis and reaction with OH and O3 are very likely valid to a broader class of compounds which are important intermediates in the oxidation of isoprene and (no doubt) many other compounds.

General comment

Among several interesting findings, this study provides sound evidence that the interaction between the two chromophores in a nitrooxy enal enhances its absorption cross section as well as its photolysis quantum yield, so much so that photolysis is their dominant sink in atmospheric conditions around mid-day. This view was proposed as a general trait for alpha- and beta-nitrooxy carbonyls (Muller et al., 2014), based on the laboratory observation of strongly enhanced photolysis rates (compared to nonconjugated carbonyls) for several keto-nitrates (Suarez-Bertoa et al., 2012) and for several compounds including ethanal nitrate, the simplest aldehyde nitrate (Muller et al., 2014). That this enhancement also exists for nitrooxy enals (or enones) was previously proposed, but lacked experimental proof, which is provided here. The conjugated nature of the compound under consideration is very important given the distinct features of photolysis parameters of enals or enones compared to other carbonyls, and I think this aspect should be acknowledged in the manuscript. Because of very low quantum yields (ca. 0.004), the photolysis of MACR and MVK is almost negligible in spite of their very high cross sections above 300 nm. The presence of the nitrate group is found to increase the quantum yield by two orders of magnitude, to a value of the order of unity (0.28-0.48 in this study). On top of that, the cross sections are also enhanced, as nicely shown in this work. Overall, the presence of the ONO2 group has a much more dramatic impact for the photolysis rates of enals (or enones) than for other carbonyls. For this reason, I recommend that the studied compound should be referred to as an enal in the title and in the abstract.

We have changed to refer to this compound as “isoprene nitrooxy enal”, or “nitrooxy enal”, in the title, abstract and the rest of the manuscript.

In addition, the article presents an experimental determination of the OH- and O3- reaction rates of the nitrooxy enal, thereby enabling the estimation of the relative contribution of photolysis and reaction with OH and O3 to the total photochemical sink of this compound. Photolysis is found to be generally dominant during the day. The further degradation mechanism following photolysis or reaction with OH is also explored, and yields of different products are derived. Photolysis is believed to proceed in part C2 by O–NO2 dissociation, as proposed in Muller et al. (2014), and for some part by C– CHO scission. Interpretation of the CIMS measurements and the derivation of yields is helped by kinetic modelling to account for the losses of the main observed products. The only reservation I have concerns the choice of photolysis rates for those products in this analysis

(see further below). But this is only a minor issue which should not affect the main conclusions of the study. I therefore recommend publication in ACP, after the authors take the above considerations into account, and address the following comments.

Minor comments

lines 71-78: The interaction between chromophores in nitrooxy carbonyls (i.e. also aldehydes) was found to enhance not only the cross sections but also the quantum yields (Muller et al., 2014). The combined effects on cross sections and quantum yields were observed for ethanal nitrate and for the sum of methyl vinyl ketone nitrate and methacrolein nitrate (MVKNO3 + MACRNO3) of which the measured temporal evolution in the experiment of Paulot et al. (2009) provided constraints on the photolysis parameters. A quantum yield of the order of unity was also proposed for the major nitrooxy enal produced in the oxidation of isoprene by NO3. Its estimated photolysis rate was 5.6 x 10−4 s −1 for a solar zenith angle of 30 degrees, assuming a unity quantum yield and using the cross sections of MACR. As a consequence, photolysis was estimated to outrun OH-oxidation in atmospheric conditions.

On lines 73-80 of the revised manuscript, we have added more clarification on the results reported by the Muller et al. (2014) study, to indicate that the interaction between chromophores can enhance both cross section and quantum yield.

line 168: The error bar for the wall loss rate constant appears somewhat optimistic in view of the scatter shown on Fig. 6. How was it derived?

The reported error is the standard error (s) of the coefficient. For clarification, we now report the result with 95% confidence interval, using $t_{(N-2)}$*s on lines 215-216.

line 175: "... cis isomer was present". I guess you mean "... was formed from the trans isomer", correct?

We have re-worded the reasoning for this part on line 226-238.

Figure 7. The caption should tell that the cross sections of the nitrate were obtained in acetonitrile.

We have included this information in the caption.

line 239: Is the factor 1.7 an average weighted by the irradiance spectrum?

The factor 1.7 is not a weighted average. It is calculated as the average ratio of gas-phase cross section divided by condensed-phase cross section at each wavelength. This is clarified on lines 296-298.

lines 393: Using the photorate of the 4,1-carbonyl nitrate to represent the photolysis loss of ethanal nitrate and the MVK nitrate is not appropriate as those compounds are not conjugated and their absorption cross sections are expected to be much lower in the relevant wavelength range (300-400 nm). For MVKNO3, I recommend to use the cross sections of 3-nitrooxy-2-butanone which are known from Barnes et al. (1993), and a quantum yield of unity since this choice led to best results for MVKNO3+MACRNO3 evolution in Muller et al. (2014). For ethanal nitrate, the cross sections shown in Fig. 2 in Muller et al. (2014) could be used, as it was also found to give good results against Paulot et al. This update should decrease the calculated photolysis frequencies, especially for MVKNO3. Note that the OH-reaction rate of MVKNO3 according to Kwok and Atkinson (1995) is 1.3 x 10−12 cm3 molec−1 s −1 , which might not be entirely negligible.

We calculated the photolysis frequency of 3-nitrooxy-2-butanone using the cross section reported by Barnes et al. (1993) and a unity quantum yield. The result, 4.5E-6 s^{-1} is used as a surrogate for the photolysis frequency of MVKNO3. We calculated the MVKNO3 + OH rate constant as 1.78E-12 $cm^3molec^{-1}s^{-1}$, based on Kwok and Atkinson (1995). We corrected the MVKNO3 yield using these updated loss rates on lines 468-481.

We calculated that the photolysis frequency for ethanal nitrate is 1.69E-5 s^{-1}, using the cross section recommended by Muller el al (2014) and a unity quantum yield. This information is added on lines 464-466.

line 494: As far as photolysis is concerned, I don't really see why unsaturated ketones would be much different from unsaturated aldehydes. The absorption cross sections and quantum yields of MVK and MACR are very similar.

The unsaturated ketones and aldehydes are expected to have similar photochemical properties, given their similar structures, but the ketones may not be as reactive to OH as the aldehydes. We have made the clarification on lines 583-587.

Technical corrections
line 106 "derived"
line 213: "were known" –> "are known"
line 214: "we calculated" –> we calculate"

line 220: "introduced" –> "introduce"
line 226: "we calculated that lambda0 was..." –> "we calculate that lambda should be..."
line 273: "multiplying by..."

The above corrections have been made.

References

Barnes, I., Becker, K. H., and Zhu, T.: Near UV absorption spectra and photolysis products of difunctional organic nitrates: Possible importance as NO x reservoirs, Journal of Atmospheric Chemistry, 17, 353-373, 10.1007/bf00696854, 1993.
Kwok, E. S. C., and Atkinson, R.: Estimation of hydroxyl radical reaction rate constants for gas-phase organic compounds using a structure-reactivity relationship: An update, Atmospheric Environment, 29, 1685-1695, http://dx.doi.org/10.1016/1352-2310(95)00069-B, 1995.
Müller, J. F., Peeters, J., and Stavrakou, T.: Fast photolysis of carbonyl nitrates from isoprene, Atmospheric Chemistry and Physics, 14, 2497-2508, 10.5194/acp-14-2497-2014, 2014.

The manuscript, "Photochemical degradation of isoprene-derived 4,1-carbonyl nitrate" by Xiong et al. reports on the photolysis rate of the trans-4-1 carbonyl nitrate derived in the atmosphere from the NO3 radical oxidation of isoprene. The manuscript is well written and describes a great deal of well-thought-out work. The main implication of this work is that this conformer of isoprene carbonyl nitrate will have a short lifetime in the atmosphere due mainly to photolysis, with non-negligible contribution from OH oxidation. The work also identifies some of the major byproducts of OH oxidation and photolysis of this compound, thereby improving our understanding of isoprene photochemistry. The work should be published in ACP with a few minor clarifications.

Minor questions/comments/suggestions: I disagree with the "double" and "single" exponential discussion (lines 175-178). That a double exponential will be observed if large amounts of cis is present is unconvincing without additional information and likely cannot be concluded without knowing the isomerization rate. What is the chamber residence time? A cis-trans equilibrium at some point will be reached. If the rate at which this occurs is instantaneous (or at least much faster than residence time), a single exponential will always be observed because the CIMS only ever sees a mixture of the two isomers. Would you expect a significant difference in the photolysis rate of cis versus trans? If not, does it matter which isomer you are measuring? All that matters for this part of the experiment is the decay rate. If photo lifetime of cis versus trans is very different, you would have to qualify that the 1.3e-5 sec-1 rate is some average of the two isomers.

The chamber is operated in a static rather than dynamic mode. The duration of each experiment is about 3 hours. If a cis-trans equilibrium is established instantaneously, a single exponential will be observed. However, we don't expect the cis and trans isomer to differ in photolysis frequency, given they both have the nitrooxy enal structure. Therefore, the measured decay rate should represent the photolysis frequency of the trans precursor in the reaction chamber. We have added this discussion to lines 226-238.

It would be helpful to know which compounds whose structures are drawn in figures 10 and 15, as well as those boxed in figures 11 and 12 are observed by both GC and CIMS. The CIMS captures signal at nominal masses, therefore, to infer not only molecular composition (CxHyOz) but molecular structure (i.e. identifying functional groups) would impart a certain amount of uncertainty. If only the CIMS without GC is used to infer a compound identity (such as dinitrates which I imagine do not survive GC column), this is worth clarifying. Also, how well can you distinguish MVK nitrate from MACR nitrate with GC /CIMS?

The compounds that were observed by both GC and CIMS are now indicated in blue. The structures proposed in figures 10-12 and 15-16 are inferred based on nominal masses. We have added this information to the captions of these graphs.

We are unclear how well the GC/CIMS can distinguish MVK nitrate from MACR nitrate. For this work, we do not expect to have MACR nitrate in the system, because the nitrooxy enal has a secondary carbon at its C3 position, and the OH oxidation reaction cannot add a functional group at this position while still maintaining it as a secondary carbon as in MACR nitrate. Therefore, we infer m/z 276 to be MVK nitrate. We have added this discussion to lines 409-412.

Given CIMS observations of boxed compounds in figures 12 and 16, can you infer branching ratios of OH oxidation paths (a versus b in figure 12) and the two photolysis paths (figure 16).

The branching ratios for the OH oxidation cannot be obtained because the products from H-abstraction pathway were not quantified. For the OH addition pathway, we did quantify two of the products. However, ethanal nitrate is produced from both H abstraction and OH addition pathways (including both (a) and (b) pathways). MVK nitrate is produced in pathway (b) only, but it has ethanal nitrate as byproduct (along with C5 dinitrate), which makes it impossible to determine the branching ratio for pathway (b). We have added this discussion to lines 491-497.

For photolysis pathways, we cannot determine the branching ratio because the photolysis products were identified, but not quantified. This is clarified on lines 549-552.

How were the spectra in figure 3 obtained? Are they of three different samples, one containing pure carbonyl nitrate in solvent, the second pure MACR, and the third pure isopropyl nitrate? If the spectra are of one mixture containing all three compounds, how were the spectra distinguished or attributed to a particular compound?

The spectra were obtained with three different samples, each one containing one pure solute in the acetonitrile solvent. This is clarified on line 99-100.

Is each a simulated or calculated spectrum from the observed (the sum of the three spectra shown in figure 3). This needs to be better explained, in particular, for the discussion on lines 142 to 165. This discussion tries to establish that the excitation features of carbonyl nitrate is well understood, that the one near 255 nm is from the nitrate group C2 and the one near 330 nm is from the aldehyde group. However, there are some aspects of this discussion that are difficult to follow, hence, the argument is not as convincing as can be. For instance, figure 3 shows isopropyl nitrate along with MACR and carbonyl nitrate, whereas figure 4 shows n-butyl nitrate. Explain why the combination of these 3 compounds was chosen for this part of the study...similarity in structure, overlapping functional groups, etc. Figure 4 and 5 involve calculations...why not include isopropyl nitrate as well? It would make comparison simpler and argument more convincing.

The calculation was performed for each spectrum separately. In Fig. 3, we compared isopropyl nitrate and MACR with isoprene nitrooxy enal, because MACR has the enal structure, and isopropyl nitrate has the nitrooxy group, and the combination of these two compounds resembles the nitrooxy enal studied in this work. This explanation was added to lines 102-105 of the revised manuscript.

To better compare the measured UV spectra with the calculated spectra, we have now added calculations for isopropyl nitrate in section 3.2 and 4.1 of the revised manuscript.

Figure 4 is described as an absorption spectrum. But it looks very different from figure 3. Figure 4 looks more like band strength or absorption lines. Is it possible to simulate actual absorption spectra (one for MACR, one for carbonyl nitrate, one for n-butyl nitrate) given data shown in figure 4 under conditions similar to those in figure 3 and compare that result to figure 3? Would provide stronger support to TDDFT calculation.

Fig. 4 shows the theoretical gas phase absorption spectra of the nitrooxy enal, MACR, isopropyl nitrate, and n-butyl nitrate. To accurately capture the broadening of these lines in TDDFT, it is required to consider the effect of the chromophore's vibrational degrees of freedom and/or to include a condensed phase environment that surrounds the chromophore. However, explicit modeling of broadening either due to vibronic interactions or solvent effects is computationally challenging. We believe the analysis of this kind is beyond the scope of the present work. It is also possible to artificially broaden stick spectra with Gaussian or Lorentzian envelopes, to represent collision broadening. However, we do not think that such artificial broadening would provide any additional information, while the presented stick theoretical spectra provide adequate support for our arguments. This discussion is added to lines 165-170.

Lines 142-144, reads as if authors are saying there is a transition for n-butyl nitrate near 330 nm when there is not. Please re-word.

We have re-worded the sentence to refer the 330 nm transition as a transition for the nitrooxy enal only on line 180-182.

Lines 148-149..."...Earth's surface..." what is the significance of this statement? Figure 5 and lines 159-165. What is the relevance of including the excitation feature near 210 nm (figure 4) when there is no experimental data (figure 3) to compare against. This spectral region is also "beyond atmospheric relevance" as authors note.

The theoretical calculations suggest that the nitrooxy group has an electronic transition at 210 nm and 255 nm, but both wavelengths are outside the solar radiation spectrum near the surface. Therefore, we speculate that the isoprene nitrooxy enal absorbs photons primarily through the transition of the enal chromophore, instead of the nirooxy functionality, and the dissociation of the $O{-}NO_2$ bond likely results from intramolecular energy redistribution. This discussion is added to line 207-212.

Including those transitions gives a clear picture of how the theoretical spectrum of the nitrooxy enal is a function of both nitrooxy absorption and absorption of the enal group, through the comparison with the absorption of the alkyl nitrates and MACR. While though they might not seem directly relevant to the experimental data, they show internal consistency of the simulated spectra. This discussion is further clarified on line 198-200.

Figure 1. Is the reaction between the NO3 radical and nitroxy peroxy radical the only route to the alkoxy radical, hence carbonyl nitrate? Isn't reaction with RO2 more likely than NO3 to generate the alkoxy given abundance of RO2 in most BVOC rich region? At the very least, RO2 should be included. Rollins et al 2009 ACP (www.atmos-chemphys.net/9/6685/2009/).

We have now included RO_2 as a second reactant to form nitrooxy alkoxy radicals in Fig. 1.

Application to field observation was demonstrated in figure 9. Out of curiosity, is there direct observation of isoprene carbonyl nitrate from the field using CIMS+GC? Spectrum or chromatogram or time series or diel average? How abundant is isoprene carbonyl nitrate considering it is produced at night when loss rate is presumably slow? How well can the CIMS distinguish C5H7NO4 from potential interference due to the isotope of the signal at mz 271. Do you have carbonyl nitrate + NO3 oxidation results, similar to those of OH and photolysis shown here? These would be nice additions to this work, but perhaps saving for separate manuscript.

To date there is no report on field observations of isoprene carbonyl nitrates using CIMS or GC method. One of the challenges for this type of measurement might be that when iodide-based CIMS is used, the isoprene nitrooxy enal can react with iodide and form NO_3^-, instead of nitrate-iodide cluster, and the nitrooxy enal could be detected as NO_3 and N_2O_5 radicals. In addition, iodide-based CIMS is most sensitive to species with acidic hydrogens, which the enal nitrate does not have. Brown et al. (2009) observed NO_3 + isoprene chemistry in Northeast US in the 2004 NEAQS study, and they estimated that the total concentrations of the isoprene-derived nitrate could reach 500 ppt. The carbonyl nitrates are expected to contribute a significant fraction to the total organic nitrates estimated by Brown et al. (2009), but the exact amount cannot be obtained without direct measurement of the carbonyl nitrates. This discussion is added to lines 434-440.

Our CIMS has unit mass resolution. For this work, we used pure isoprene nitrooxy enal as the precursor, which did not introduce much interference at m/z 271. This is clarified on lines 122-124.

Since this work is focused on the photochemistry of the nitrooxy enal, which describes the loss-dominant processes after sunrise, we did not include experiments concerning NO_3 oxidation. This is clarified on lines 116-118 of the revised manuscript.

Figure 4. Many have a difficult time distinguishing red from blue. May help to choose different color scheme. Also, are vertical lines necessary to show this data? The three lines at 210 nm are difficult to distinguish from one another. Perhaps use markers instead? Also, change "1×10^exponent" to just "10^exponent"

Fig. 4 was updated including the changes suggested by the reviewer.

The wall loss rate constant is fairly high compared to the photolysis rate constant. What is the residence time in the 5.2 m long tubing? Is laminar flow maintained? Also, curious if heating the inlet to 50 degC can induce cis-trans isomerization.

The wall loss and photolysis rate constants were obtained with repeated experiments. The radiation inside the chamber is approximately 10% of solar radiation. Therefore, our photolysis rate constant is small, making the wall loss rate constant high compared with photolysis frequency. This information is added to line 218-220.

The residence time in the tubing is around 5 s, and laminar flow is maintained. We have conducted inlet tests for the heated tubing, and we do not expect significant isomerization inside our sampling line. This information is added to line 125-131.

Line 235. Why is there no gas phase spectrum? Is it technically challenging? If so, it would be helpful for community to know.

We were concerned about potentially large wall loss of the organic nitrate inside a small UV cell. Hence, the measurements were performed with nitrate solutions. This is clarified on line 100-102.

Reference

Brown, S. S., deGouw, J. A., Warneke, C., Ryerson, T. B., Dubé, W. P., Atlas, E., Weber, R. J., Peltier, R. E., Neuman, J. A., Roberts, J. M., Swanson, A., Flocke, F., McKeen, S. A., Brioude, J., Sommariva, R., Trainer, M., Fehsenfeld, F. C., and Ravishankara, A. R.: Nocturnal isoprene oxidation over the Northeast United States in summer and its impact on reactive nitrogen partitioning and secondary organic aerosol, Atmos. Chem. Phys., 9, 3027-3042, 10.5194/acp-9-3027-2009, 2009.

Photochemical Degradation of Isoprene-derived ~~4,1-Carbonyl Nitrate~~4,1-Nitrooxy Enal

F. Xiong[1], C. H. Borca[1], L. V. Slipchenko[1] and P. B. Shepson[1,2]

[1] Department of Chemistry, Purdue University, West Lafayette, IN

[2] Department of Earth, Atmospheric and Planetary Sciences, Purdue University, West Lafayette, IN

Correspondence to: P. B. Shepson (pshepson@purdue.edu)

Abstract

In isoprene-impacted environments, carbonyl nitrates are produced from NO_3-initiated isoprene oxidation, which constitutes a potentially important NO_x reservoir. To better understand the fate of isoprene carbonyl nitrates, we synthesized a model compound, *trans*-4-nitrooxy-2-methyl-2-buten-1-al (4,1-isoprene carbonyl nitrate, or 4,1-isoprene nitrooxy enal) and investigated its photochemical degradation process. The measured OH and O_3 oxidation rate constants (298 K) for this ~~carbonyl nitrate~~nitrooxy enal are $4.1(\pm0.7)\times10^{-11}$ cm^3 $molecules^{-1}$ s^{-1} and $4.4(\pm0.3)\times10^{-18}$ cm^3 $molecules^{-1}$ s^{-1}, respectively. Its~~The~~ UV absorption spectrum ~~of the carbonyl nitrate~~ was determined, and the result is consistent with TDDFT calculations. Based on its UV absorption cross section and photolysis frequency in a reaction chamber, we estimate that the ambient photolysis frequency for this compound is $3.1(\pm0.8)\times10^{-4}$ s^{-1} for a solar zenith angle (SZA) of 45°. The fast photolysis rate and high reactivity toward OH lead to a lifetime of less than one hour for the ~~carbonyl nitrate~~isoprene nitrooxy enal, with photolysis being a dominant daytime sink. The nitrate products derived from the OH oxidation and the photolysis of the ~~isoprene~~ nitrooxy enal~~carbonyl nitrate~~ were identified with an iodide-based chemical ionization mass spectrometer (CIMS). For the OH oxidation reaction, we quantified the yields of two nitrate products, methyl vinyl ketone (MVK) nitrate and ethanal nitrate, which together contributed to ~~37~~36(±5)% of the first-generation products.

1 Introduction

Over the past century, tropospheric background ozone concentrations have increased from around 20 ppb to ~40 ppb, with urban-impacted concentrations often rising to 60-100 ppb (Parrish et al., 2014; Vingarzan, 2004), posing harmful effects on human health and crop yields (Lefohn and Foley, 1993; Lippmann, 1989). Tropospheric ozone is catalytically produced in the chemical reactions of nitrogen oxides ($NO_x \equiv NO + NO_2$) and volatile organic compounds (VOCs) (Haagen-Smit, 1952). NO_2 photolysis forms ozone (Blacet, 1952), and the ozone production rate is enhanced when the NO-NO_2-O_3 cycle is coupled with the oxidation of VOCs (Chameides et al., 1988; Chameides and Walker, 1973; Chameides et al., 1992). When NO_x is incorporated into organic molecules and forms organic nitrates ($RONO_2$), however, ozone formation is suppressed (Roberts, 1990). Organic nitrates are a temporary NO_x reservoir. Degradation of organic nitrates can release NO_2 back into the atmosphere (Aschmann et al., 2011), and thus facilitate ozone production. Organic nitrates in the gas phase can also adsorb onto atmospheric aerosols, followed by condensed-phase hydrolysis (Rindelaub et al., 2015). This process removes the reactive nitrogen from the atmosphere permanently, as the nitrooxy group is ~~turned~~ converted into the non-volatile NO_3^- ion (Darer et al., 2011; Hu et al., 2011). The relative importance of these parallel nitrate sinks affects the availability of NO_x and the ozone production rate in the troposphere. Therefore, detailed understanding of the loss mechanisms of organic nitrates is crucial to understanding the dynamics of ground-level ozone formation.

Modeling studies suggest that isoprene-derived organic nitrates have substantial influence on the NO_x cycle and tropospheric O_3 production (Horowitz et al., 2007; Mao et al., 2013; Paulot et al., 2012; Wu et al., 2007). During the daytime, isoprene is lost rapidly to OH oxidation, forming organic nitrates through the RO_2 + NO reaction, with a yield of 7-14% (Lockwood et al., 2010; Patchen et al., 2007; Paulot et al., 2009; Sprengnether et al., 2002; Tuazon and Atkinson, 1990; Xiong et al., 2015). At night, reaction with NO_3 is a significant removal pathway for isoprene (Brown et al., 2009; Starn et al., 1998), and organic nitrates constitute 65-70% of the oxidation products (Perring et al., 2009; Rollins et al., 2009). While NO_3-initiated isoprene oxidation contributes to a small fraction of isoprene loss, this reaction pathway could generate approximately half of the isoprene-derived organic nitrates on a regional scale, due to its large nitrate yield (Horowitz et al., 2007; Xie et al., 2013).

Fig.1 shows the formation pathways of organic nitrate products from NO_3-initiated oxidation of isoprene, including hydroperoxy nitrate, carbonyl nitrate and hydroxy nitrate. Reactions for only one of the nitrooxy peroxy radicals are shown for brevity. The hydroxy nitrates can be also formed in the OH-initiated isoprene oxidation reactions, and their production and degradation have been studied extensively in both laboratory and field studies (Chen et al., 1998; Giacopelli et al., 2005; Grossenbacher et al., 2004; Jacobs et al., 2014; Lee et al., 2014b; Lockwood et al., 2010; Patchen et al., 2007; Paulot et al., 2009; Sprengnether et al., 2002; Tuazon and Atkinson, 1990; Xiong et al., 2015). For the hydroperoxy nitrates, Schwantes et al. (2015) investigated their production from the $RO_2 + HO_2$ reaction and identified the nitrooxy hydroxyepoxide product from the OH oxidation of the isoprene hydroperoxy nitrate. For the isoprene carbonyl nitrates, their formation has been quantified in an experimental study (Kwan et al., 2012), but their sinks and fate can only be inferred from analog molecules, such as nitrooxy ketones, due to lack of direct studies on these specific compounds. Suarez-Bertoa et al. (2012) conducted kinetics experiments on three synthesized saturated nitrooxy ketones, and their results indicate that photolysis is the dominant sink for these nitrate compounds. By comparing the published UV absorption spectra of α-nitrooxy ketones with the UV spectra of the mono-functional nitrates and ketones, Müller et al. (2014) suggested that the nitrooxy ketones have enhanced absorption cross sections, due to the interaction between the –C=O and the $–ONO_2$ chromophores. In addition, near-unit photolysis quantum yields for α-nitrooxy acetone and 3-nitrooxy-2-butanone were inferred by Müller et al. (2014), based on the photolysis frequencies determined by Suarez-Bertoa et al. (2012) and known absorption cross sections (Barnes et al.). The enhanced absorption cross sections and quantum yields of carbonyl nitrates resulting from chromophore interactions lead to fast photolysis rates that are more consistent with the loss rates constrained by the measured temporal profiles of carbonyl nitrates in an isoprene oxidation experiment performed by Paulot et al. (2009) (Müller et al., 2014). ~~, which can facilitate the dissociation of the O−NO_2 bond~~. Like the ~~nitrooxy ketones~~carbonyl nitrates discussed by Suarez-Bertoa et al. (2012) and Müller et al. (2014), some of the carbonyl nitrate isomers derived from NO_3 + isoprene oxidation ~~has~~ have a conjugated chromophore, −C=C−C=O (enal), at the β position of the nitrate group, which may enhance the UV absorption cross section of the molecule and facilitate its photolytic dissociation. However, since the five-carbon isoprene carbonyl nitrate (nitrooxy enal) (Fig. 1) is unsaturated, it is also expected to be lost rapidly to OH oxidation. To date, the relative importance of the individual photochemical sinks for the

unsaturated carbonyl nitrates is still unclear. To answer this question, we synthesized a model compound for the five-carbon isoprene carbonyl nitrates, and investigated its photochemical reactivities and fate.

2 Synthesis and characterization

A model compound, ~~4,1-isoprene carbonyl nitrate (~~*trans*-2-methyl-4-nitrooxy-2-buten-1-al (4,1-isoprene nitrooxy enal) was synthesized following the reaction scheme in Fig. 2. The nitrate was prepared by reacting $AgNO_3$ with the corresponding bromide (*trans*-4-bromo-2-methyl-2-buten-1-al) (Ferris et al., 1953), which was synthesized following Gray (1981). The ^{1}H and ^{13}C NMR spectra of the synthesized product are shown in Fig. S1 and Fig. S2. Its IR absorption spectrum is shown in Fig. S3.

Shown in Fig. 3 are the UV absorption cross sections for the ~~carbonyl nitrate~~nitrooxy enal, methacrolein (MACR) and isopropyl nitrate.~~,~~ Each spectrum was obtained using a solution that contained one single pure analyte in acetonitrile solvent. Only solution-phase spectra were determined, because gas-phase cells may have potential wall loss problems and thus the quantitative gas-phase cross sections are difficult to measure. We compared isopropyl nitrate and MACR with isoprene nitrooxy enal, because MACR has the enal structure, and isopropyl nitrate has the nitrooxy group, and the combination of these two compounds helps to illustrate the absorption features of the nitrooxy enal studied in this work. The absorption cross section of the carbonyl nitrate is enhanced relative to that of MACR, but the two spectra have similar features from 320 nm to 400 nm with peak absorption at 325 nm. This is probably because they both contain the O=C–C=C chromophore. Below 320 nm the absorption of the ~~carbonyl nitrate~~nitrooxy enal is enhanced significantly in comparison with that of isopropyl nitrate. This observation is consistent with reports from Müller et al. (2014) that molecules containing α,β-nitrooxy ketone functionalities have enhanced UV absorption.

Formatted: Font color: Auto

3 Methods

3.1 Setup for the kinetics chamber experiments

Three sets of reaction chamber experiments were conducted to determine the photolysis frequency, OH oxidation rate constant and the O_3 oxidation rate constant for the ~~carbonyl nitrate~~isoprene

nitrooxy enal. Since this work is focused on the photochemistry of the nitrooxy enal, which describes the loss-dominant processes after sunrise, we did not include experiments concerning the NO_3-initiated oxidation processes for this compound. The experiments were performed in the 5500 L Purdue photochemical reaction chamber (Chen et al., 1998). A chemical ionization mass spectrometer (CIMS) with I^- as the reagent ion (Xiong et al., 2015) was used to quantify the ~~carbonyl nitrate~~nitrooxy enal (observed at nominal mass m/z 272) and its nitrate degradation products ~~(Xiong et al., 2015)~~. The CIMS has unit mass resolution. Since pure isoprene nitrooxy enal was introduced into the reaction as the precursor, we do not expect significant interference from the isotope signal of m/z 271. The chamber air was sampled into the CIMS through ~~a~~ 5.2 m long FEP tubing (0.8 cm ID, heated to constant 50 °C). The residence time for the sampling tubing was approximately 5 s, and laminar flow was maintained. To assess the influence of the heated inlet on the stability of the nitrooxy enal, we have sampled the nitrooxy enal using the heated 50 °C inlet and using a 20 cm room temperature inlet, and there was no significant difference in their corresponding CIMS signals. In addition, the *trans*-isoprene nitrooxy enal was synthesized in an oil bath maintained at 70 °C, but the formation of the *cis* isomer was not observed. Therefore, we do not consider that there is significant thermal isomerization inside our sampling line. The photolysis frequenecy was obtained by measuring the loss of the ~~carbonyl nitrate~~nitrooxy enal inside the reaction chamber in the presence of UV radiation and propene as a radical scavenger. When the UV lamps were turned off, the wall loss rate constant for the ~~carbonyl nitrate~~nitrooxy enal was derived~~dervied~~ by observing its slow decay, with propene as an ozone and NO_3 scavenger. The OH reaction rate constant and O_3 reaction rate constant were obtained using the relative rate method (Atkinson and Aschmann, 1985). Propene was used as the reference compound, and its changing concentrations were measured using a GC-FID equipped with a 0.32 mm Rtx-Q-Bond column. For the OH oxidation experiments, OH was generated through the photolysis of isopropyl nitrite, which was synthesized foll~~w~~owing Noyes (1933). NO was added to the chamber to suppress the formation of O_3. In addition, two OH oxidation experiments were performed without propene in order to quantify the oxidation products. For the OH-initiated oxidation experiments, NO and NO_2 were measured using the Total REactive Nitrogen Instrument (TRENI) (Lockwood et al., 2010). The ozonolysis experiments were performed in the dark, and cyclohexane was added to the chamber as an OH scavenger. The initial conditions for the experiments are listed in Table S1.

Formatted: Font color: Auto

Formatted: Font color: Auto

Formatted: Font color: Auto

Formatted: Font: Italic, Font color: Auto

Formatted: Font color: Auto

Formatted: Font: Italic

Formatted: Font color: Auto

3.2 Computational methods

The theoretical UV absorption spectra of the ~~carbonyl nitrate~~isoprene nitrooxy enal, MACR, isopropyl nitrate and *n*-butyl nitrate in the gas phase were calculated separately and analyzed, in four stages, using time-dependent density functional theory (TDDFT~~;~~ (Hohenberg and Kohn, 1964; Kohn and Sham, 1965; Runge and Gross, 1984)). All calculations were carried out using the computational chemistry package Q-Chem 4.3 (Shao et al., 2015). First, the structure of each molecule was optimized employing the long-range corrected hybrid density functional ωB97X-D (Chai and Head-Gordon, 2008) with the 6-31+G* basis set (Frisch et al., 1984). A high accuracy grid was employed. Second, frequenc~~ies~~y calculations were executed on the optimized structures to verify their accuracy. These were run using the same setup described above. Third, after assuring the structures represented adequate minima, the first ten singlet excited states of each molecule were computed with TDDFT, using the same functional and basis set. Finally, a visual analysis of the molecular orbitals (MOs) was carried out with the visualization software IQmol 2.7 (Gilbert, 2012).

4 Results

4.1 Absorption spectra and density functional calculations

Fig. 4 shows the TDDFT UV absorption spectra of the ~~carbonyl nitrate~~nitrooxy enal, MACR, isopropyl nitrate and *n*-butyl nitrate. There are three groups of transitions in the simulated spectra. Unlike the absorption bands depicted in Fig 3, the theoretical gas-phase spectra in Fig. 4 are showing only the electronic transition lines. To accurately capture the broadening of these lines in TDDFT so as to simulate absorption bands, we have to consider the effect of the chromophore's vibrational degrees of freedom and/or to include a condensed phase environment that surrounds the chromophore. However, explicit modeling of broadening either due to vibronic interactions or solvent effects is computationally challenging and beyond the scope of this work.

Formatted: Font color: Auto

Both MACR and the ~~carbonyl nitrate~~nitrooxy enal show a relatively weak transition in the region around 330 nm, which corresponds to the first electronic transition, from the highest occupied molecular orbital (HOMO) to the lowest unoccupied molecular orbital (LUMO), in both molecules.

Fig. 5a provides comparative information between the first electronic transition of the ~~carbonyl nitrate~~nitrooxy enal and the homologous excitation of MACR. As shown in Fig. 5a the character of the molecular orbitals involved in this transition is similar in both cases, indicating that the aldehyde group is involved in the first electronic excitation of the ~~carbonyl nitrate~~nitrooxy enal.

Fig. 5b shows the information corresponding to the second electronic transition of the ~~carbonyl nitrate~~nitrooxy enal and its~~the~~ homologous excitation in~~of~~ isopropyl nitrate and *n*-butyl nitrate. ~~Both~~ These three transitions are found in the region around 255 nm. The second electronic transition of the nitrooxy enal is 3 orders of magnitude weaker than its first excitation, located at 330 nm.~~, and they are 3 orders of magnitude darker than those at 330 nm.~~ Inspection of the character of the MOs involved in these processes reveals a correspondence between the second electronic excitation of the ~~carbonyl nitrate~~nitrooxy enal, HOMO−2 → LUMO+1, and the HOMO → LUMO transitions in both isopropyl nitrate and~~of~~ *n*-butyl nitrate. As with the previous case, that observation confirms that the nitrate group is involved in the second electronic excitation of the ~~carbonyl nitrate~~nitrooxy enal~~, but at wavelengths shorter than present at the Earth's surface~~. Fig. 5b also shows that in this case, the local character of the MOs involved in the transition is even more pronounced, with bulky lobes placed mainly over the nitrate group.

Even though the second electronic transition of carbonyl nitrate is not displayed in the experimental spectra of Fig. 3, because its range covers from 280 nm to 410 nm, it is reasonable to assume that it is caused by the local excitation of the nitrate group, based on the computational results. Thus, it can be suggested that the experimental UV absorption spectrum~~a~~ of isopropyl nitrate is comparable to those~~that~~ of isopropyl nitrate and *n*-butyl nitrate simulated computationally. Thus it is possible that the feature in the region around 280 nm of the ~~carbonyl nitrate~~nitrooxy enal experimental spectrum in~~of~~ Fig. 3 could be caused by a broadening of the transition located around 255 nm.

Another plausible explanation of the feature around 280 nm for the nitrooxy enal would be a broadening of its brightest transition in the modeled spectrum. It is located around 210 nm, and it is 3 orders of magnitude brighter than the one at 330 nm. In that region,

~~The brightest transition in the modeled spectra of the carbonyl nitrate, 3 orders of magnitude brighter than the ones at 330 nm, is located around 210 nm.~~ ~~T~~there are two transitions ~~in this region~~

and each one has a homologous excitation: the HOMO−1 → LUMO in ~~carbonyl nitrate~~nitrooxy enal is similar to HOMO−1 → LUMO in MACR, and the HOMO−5 → LUMO+1 in ~~carbonyl nitrate~~nitrooxy enal is related to the (mainly) HOMO−1 → LUMO transitions of isopropyl nitrate and *n*-butyl nitrate. These transitions are beyond the range of the experimental spectra on Fig. 3 and beyond the atmospherically relevant absorption wavelengths. The theoretical calculations suggest that the nitrooxy group has electronic transitions at 210 nm and 255 nm, but both wavelengths are outside the solar radiation spectrum near ground. Therefore, we speculate that the isoprene nitrooxy enal absorbs photons primarily through the first electronic transition concerning the enal chromophore, instead of the nirooxy functionality, and the dissociation of the O−NO_2 bond (Sect. 4.3.2) likely results from intramolecular energy redistribution.

4.2 Photochemical sinks of ~~4,1-carbonyl nitrate~~the 4,1-isoprene nitrooxy enal

Fig. 6 shows the first-order wall loss and photolysis loss of the ~~carbonyl nitrate~~nitrooxy enal inside the reaction chamber. The wall loss rate constant was 1.3(±0.~~1~~2)×10^{-5} s^{-1} (95% confidence interval), and the photolysis rate constant was 3.0(±0.~~1~~2)×10^{-5} s^{-1} (95%), after subtracting the wall loss rate constant from the first-order decay rate constant measured for the photolysis experiments. The radiation intensity inside the chamber is approximately 10% of solar radiation. Therefore, our photolysis rate constant is small, making the wall loss rate constant significant, compared with the photolysis frequency. It is worth mentioning that our reactant ~~carbonyl nitrate~~nitrooxy enal has a *trans* configuration, and it may photo-isomerize into the *cis* configuration, which would be detected at the same m/z by the CIMS. The *cis*-~~carbonyl nitrate~~nitrooxy enal can either photo-dissociate or isomerize to re-form the *trans* isomer. Our previous work suggests that the CIMS is 4 times more sensitive to the *cis* configuration than the *trans* configuration (Xiong et al., 2015). ~~If a significant amount of the *cis* isomer was present, the CIMS signal should resemble a double exponential curve,~~ If the lifetime for the *trans* → *cis* reaction is comparable to the duration of the experiments (approximately 3 hours), we would expect the CIMS signal to resemble a double exponential curve, because the *cis* isomer was being produced and consumed simultaneously. This double exponential curve is not observed for the photolysis data (Fig. 6). If a *cis*-*trans* equilibrium is established instantaneously, the CIMS signal would still be a single exponential curve, which represent the loss of both isomers. However, given the similar nitrooxy enal structures for the *cis* and *trans* isomers, we do not expect their photolysis frequencies to differ significantly, so the total

Formatted: Font color: Auto

Formatted: Font color: Auto

Formatted: Font: Italic

Formatted: Font: Italic

Formatted: Font: Italic

Formatted: Font: Italic

Formatted: Font: Italic

photolysis rate constant obtained from the CIMS measurement can be used as the photolysis frequency for the individual *cis* or *trans* isomer. ~~In an extreme scenario with rapid *trans* → *cis* isomerization, the CIMS signal should increase under radiation, due to the higher sensitivity of the *cis* isomer. For our carbonyl nitrate photolysis experiments, a single exponential decay in the CIMS signal was observed, indicating insignificant contribution from the *cis* isomer. Hence,~~ Therefore, regardless of the *trans* → *cis* isomerization rate, our measured photolysis frequency should well characterize the loss rate of the ~~carbonyl nitrate~~precursor *trans*-nitrooxy enal inside the reaction chamber.

Since the UV radiation inside the reaction chamber is different from the UV radiation in the ambient environment (Fig. 7), Cl_2 was used as a reference compound to ~~extrapolate~~ translate the nitrate photolysis rate from chamber radiation to solar radiation. The photolysis decay of Cl_2 in the reaction chamber was measured with the CIMS (Neuman et al., 2010). Cyclohexane was added to the chamber to scavenge the Cl atoms so that Cl_2 was not re-formed from Cl + Cl recombination. The first-order photolysis rate constant for Cl_2 was 2.50(±0.~~04~~08)×10^{-4} s^{-1} (Fig. S4).

The photolysis frequency (J) is the integrated product of quantum yield (Φ), absorption cross section (σ, cm^2) and actinic flux (F, cm^{-2} s^{-1}) across all wavelengths (Eq. 1). Therefore, the photolysis frequencies for the ~~carbonyl nitrate~~nitrooxy enal and Cl_2 in the reaction chamber can be compared as in Eq. 2.

$$J = \int \Phi_\lambda \sigma_\lambda F_\lambda d\lambda \quad \text{(Eq. 1)}$$

$$\frac{J_{Cl_2}^{chamber}}{J_{nitrate}^{chamber}} = \frac{\sum \varphi_{Cl_2}\sigma_{Cl_2}F_{chamber}}{\sum \varphi_{nitrate}\sigma_{nitrate}F_{chamber}} \quad \text{(Eq. 2)}$$

$J_{Cl_2}^{chamber}$ and $J_{nitrate}^{chamber}$ are the photolysis frequencies of Cl_2 and the ~~carbonyl nitrate~~nitrooxy enal inside the chamber. σ_{Cl_2} and $\sigma_{nitrate}$ are the cross sections for Cl_2 and the ~~carbonyl nitrate~~nitrooxy enal at each wavelength. $\sigma_{nitrate}$ was determined by this work (Fig. 3). σ_{Cl_2} has been measured previously and the IUPAC recommended values were used (Atkinson et al., 2007). $F_{chamber}$ is the wavelength-dependent flux of photons inside the chamber. The radiation spectrum (Fig. 7) of the chamber UV lamps (UVA 340) was obtained from the manufacturer (Q-lab), but the actual absolute radiation intensity in the chamber is expected to differ from the manufacturer's radiation

Formatted: Font: Italic
Formatted: Font: Italic
Formatted: Font: Italic

spectrum by a scaling factor, because of the inverse-square dependence on distance, and our specific multi-lamp geometry. When Cl_2 was used as a reference compound for the nitrate photolysis rate, the scaling factors in Eq. 2 will cancel.

The Cl-Cl bond dissociation energy is 243 kJ/mol (Luo, 2007b), equivalent to a photon at 492 nm. Since Cl_2 has only one bond, it has unity quantum yield below 492 nm and zero quantum yield above 492 nm. The emission spectrum of the UV lamps for the reaction chamber is centered from 300 nm to 400 nm (Fig. 7). Hence, φ_{Cl_2} =1 in Eq. 2, at all wavelengths. For the ~~carbonyl nitrate~~nitrooxy enal, however, its quantum yield is affected by the bond dissociation energy, intramolecular vibrational energy redistribution and relaxation of the excited molecule from collisions, so an average effective quantum yield ($\varphi_{nitrate}^{eff}$) is assumed, and Eq. 2 becomes Eq. 3. Since the photolysis rates, absorption cross sections and chamber radiation spectrum ~~were~~ are known, we calculate~~d~~ that $\varphi_{nitrate}^{eff}$ was 0.48.

$$\frac{J_{Cl_2}^{chamber}}{J_{nitrate}^{chamber}} = \frac{\sum \sigma_{Cl_2} F_{chamber}}{\varphi_{nitrate}^{eff} \sum \sigma_{nitrate} F_{chamber}} \quad \text{(Eq. 3)}$$

The effective quantum yield of 0.48 indicates that when the ~~carbonyl nitrate~~nitrooxy enal~~s~~ absorbs a photon inside the reaction chamber, the probability (averaged across the absorption wavelengths) for it to dissociate is 48%. However, the probability for nitrate photolysis is not equal at all wavelengths, the low energy photons (long wavelength) being less likely to induce photo-dissociation. Hence, we introduce~~d~~ a threshold wavelength λ_0, for which the ~~carbonyl nitrate~~nitrooxy enal has unity quantum yield below λ_0 and zero quantum yield above λ_0. Although this approach accounts for the energy difference of photons with different wavelengths, it is still a very rough estimation. Using the threshold wavelength, the effective quantum yield can be expressed by Eq. 4 and Eq. 5, where $\varphi(\lambda)$ is the quantum yield of the ~~carbonyl nitrate~~nitrooxy enal, and $F(\lambda)$ is the chamber photon flux (Fig. 7), as a function of the wavelength λ. Solving for the unknown λ_0 in Eq. 5, we calculate~~d~~ that λ_0 ~~was~~should be 347 nm.

$$\varphi(\lambda) = \begin{cases} 1 & (\lambda \leq \lambda_0) \\ 0 & (\lambda > \lambda_0) \end{cases} \quad \text{(Eq. 4)}$$

$$\frac{\sum_\lambda F(\lambda) \cdot \varphi(\lambda)}{\sum_\lambda F(\lambda)} = 0.48 \quad \text{(Eq. 5)}$$

The solar radiation spectrum was calculated with the TUV model (Madronich and Flocke, 1998). By assuming that the ~~carbonyl nitrate~~nitrooxy enal has zero quantum yield above 347 nm and unity quantum yield below 347 nm, its photolysis frequency is 2.6×10^{-4} s^{-1} for a solar zenith angle (SZA) of 45°, and 3.7×10^{-4} s^{-1} for SZA of 0°. It is worth mentioning that the condensed-phase and gas-phase absorption spectra should be different, because the solvent molecules affect the polarization and dipole moment of the solute (Bayliss and McRae, 1954; Braun et al., 1991; Linder and Abdulnur, 1971). Although we were unable to measure the gas-phase cross section of the ~~carbonyl nitrate~~nitrooxy enal, we could assess the uncertainty caused by using the condensed-phase spectrum in our calculation, by comparing the gas-phase and condensed-phase spectra of MACR and isopropyl nitrate (Fig. S5a). On average, the gas-phase absorption cross sections of MACR and isopropyl nitrate are 1.7 times those in the solution phase (Fig. S5b), calculated as the ratio of the gas-phase cross sections divided by the condensed-phase cross sections at each wavelength. For the ~~carbonyl nitrate~~nitrooxy enal, if the gas-phase cross section is assumed to be 1.7 times that of the solution-phase cross section, the calculated effective quantum yield becomes 0.28, leading to a threshold wavelength (λ_0) of 336 nm. Using this set of cross section and quantum yields, we calculated that the nitrate photolysis frequency was 3.1×10^{-4} s^{-1} for SZA of 45°, and 4.6×10^{-4} s^{-1} for SZA of 0°, which are 19% and 24% larger than results obtained using the condensed-phase cross section. The calculated ambient photolysis frequency is not affected as significantly by the change in the absorption cross section, because it is constrained by the measured photolysis frequency in the reaction chamber. When a larger cross section is applied, a smaller quantum yield is derived, and the calculated ambient photolysis frequency, being the integrated product of the cross section, quantum yield and radiation, will not increase as much as the cross section. In addition to the cross section, our treatment of the wavelength-dependent quantum yield can also introduce uncertainty to the calculated results. If a constant effective quantum yield is used in the calculation, the ambient photolysis frequency is 2.0×10^{-4} s^{-1} for SZA of 45°, and 2.8×10^{-4} s^{-1} for SZA of 0°, which are 23% and 24% lower than assuming a threshold wavelength. Therefore, our calculated ambient photolysis frequency, based on condensed-phase absorption cross section and a threshold energy for unity quantum yield, has an uncertainty of 25%. Since we believe that the cross sections are indeed larger in the gas phase, our best estimate is $3.1(\pm0.8)\times$~~x~~10^{-4} s^{-1} for SZA=45°.

Formatted: Font color: Auto

Fig. 8 shows the results for the relative rate experiments for the OH-initiated and O_3-initiated oxidation of the ~~carbonyl nitrate~~nitrooxy enal, with propene as the reference compound. The loss of the ~~carbonyl nitrate~~nitrooxy enal to wall uptake and photolysis is corrected when comparing the oxidative loss of the nitrate to that of propene, using the same method as Hallquist et al. (1997). The OH and O_3 oxidation rate constants for propene are $3.0(\pm0.5)\times10^{-11}$ cm^3 $molecules^{-1}$ s^{-1} (Klein et al., 1984; Zellner and Lorenz, 1984) and $1.00(\pm0.06)\times10^{-17}$ cm^3 $molecules^{-1}$ s^{-1} (Herron and Huie, 1974; Treacy et al., 1992). These are the IUPAC preferred rate constants for T=298K (http://iupac.pole-ether.fr/). Hence, the OH and O_3 oxidation rate constants for the isoprene ~~carbonyl nitrate~~nitrooxy enal are, based on the results from the relative rate experiments, $4.1(\pm0.7)\times10^{-11}$ cm^3 $molecules^{-1}$ s^{-1} and $4.4(\pm0.3)\times10^{-18}$ cm^3 $molecules^{-1}$ s^{-1} respectively, at 295 K.

The OH oxidation rate constant for the ~~carbonyl nitrate~~nitrooxy enal can be estimated through the structure-activity-relationship (SAR) approach proposed by Kwok and Atkinson (1995). The rate constant for OH addition to the double bond can be calculated as k(-CH=CH), which is 8.69×10^{-11} cm^3 $molecules^{-1}$ s^{-1}, multiplied by the two correction factors C(-CHO) and C(-CH_2ONO_2), which are 0.34 and 0.47 respectively. The resulting OH addition rate constant is 1.39×10^{-11} cm^3 $molecules^{-1}$ s^{-1}. The rate constant for H abstraction from the –CHO group is 1.61×10^{-11} cm^3 $molecules^{-1}$ s^{-1}, after multiplying by a correction factor of 1 for having a double bond at its α position. The rate constant for H abstraction from the methylene group is 3.7×10^{-14} cm^3 $molecules^{-1}$ s^{-1}, calculated by multiplying the base rate constant for methylene groups, which is 9.34×10^{-13} cm^3 $molecules^{-1}$ s^{-1}, by the correction factors of the nitrate group and the double bond, which are 0.04 and 1, respectively. OH addition to the nitrate group has a rate constant of 4.4×10^{-13} cm^3 $molecule^{-1}$ s^{-1}, after taking account of the enhancement factor of 1.23 for the methylene group. H abstraction from the methyl group has a rate constant of 1.36×10^{-13} cm^3 $molecules^{-1}$ s^{-1}. By summing up the rate constants for all these reaction pathways, the SAR-derived OH oxidation rate constant for the ~~4,1 carbonyl nitrate rate constant~~isoprene nitrooxy enal is 3.1×10^{-11} cm^3 $molecules^{-1}$ s^{-1}, approximately 30% lower than the experimental measurement. The dominant reaction channels are OH addition to the double bond and H abstraction from the aldehyde group. Contributions from the other reaction pathways are small (<3%).

The relative importance of the three photochemical sinks, photolysis, OH oxidation and O_3 oxidation, depends on the solar radiation and the concentrations of OH and O_3. To better illustrate their relative contributions, observations of OH and O_3 from previous field campaigns were used to calculate the loss rates of the ~~carbonyl nitrate~~nitrooxy enal. The local solar radiation was calculated with the TUV model (Madronich and Flocke, 1998), which was then used to derive the photolysis frequency. The calculated results (Fig. 9) suggest that photolysis is a significant degradation pathway for the ~~carbonyl nitrate~~nitrooxy enal, which can dominate over OH oxidation toward mid-day. When the solar radiation intensity is small (such as 6:00 AM for the 1999 SOS campaign), OH oxidation is likely the dominant sink. Due to the fast photolysis and high reactivity toward OH, the photochemical lifetime of the ~~carbonyl nitrate~~nitrooxy enal can be as short as less than one hour.

4.3 Degradation products of the ~~4,1 carbonyl nitrate~~4,1-isoprene nitrooxy enal

4.3.1 OH oxidation

The products from the OH-initiated oxidation of the ~~4,1 carbonyl nitrate~~isoprene nitrooxy enal were observed by the CIMS. The change in the CIMS signals before and after the reaction are illustrated in Fig. 10, along with assignment of some of the molecular structures based on the molecular weight and likely chemistry. The OH-initiated oxidation reaction can proceed through two channels: H abstraction from the aldehyde group and OH addition to the double bond.

For the H abstraction pathway, a peroxyacyl nitrate (PAN) product was observed at m/z 349 (Fig. 10), which can be formed as shown in Fig. 11. The first-order dissociation rate constant for the PAN compound was determined at room temperature (295 K) using the following method. A 100 L Teflon bag containing the air mixture of approximately 1 ppm isopropyl nitrite and 30 ppb isoprene nitrooxy enal~~4,1 carbonyl nitrate~~ was irradiated, and the PAN compound was formed ~~from~~when the nitrooxy enal reacted with OH and NO_2 (produced through the photolysis of isopropyl nitrite)~~ reaction with the 4,1 carbonyl nitrate~~. After 5 min reaction time, the bag was removed from the UV radiation, and NO was injected into the bag to around 4 ppm in concentration. The bag was then sampled simultaneously by the CIMS, which monitored the decrease in the signal of the PAN compound, and by the TRENI, which monitored the concentrations of NO and NO_2. The PAN dissociation reaction is a reversible process, where the dissociation products,

peroxyacyl (PA) radical and NO_2, can re-combine to form PAN. With the addition of the large amount of NO, PA radicals are predominantly consumed by the irreversible PA + NO reaction, leading to the decay of the PAN compound. The apparent PAN dissociation rate constant can be described by Eq. 6 (Shepson et al., 1992), where k is the first-order loss rate constant measured by the CIMS (Fig. S6), k_{PAN} is the real PAN dissociation rate constant, [NO] and [NO_2] are the concentrations for NO and NO_2, and k_{NO} and k_{NO2} are the rate constants for PA + NO and PA + NO_2 reactions. Since the rate constants k_{NO} and k_{NO2} for the nitrooxy enal~~carbonyl nitrate~~-derived PA radical are unknown, the IUPAC recommended rate constants for the peroxyacetyl radicals ($CH_3C(O)O_2$) are used, with $k_{NO} = 2.0\times10^{-11}$ cm^3 $molecule^{-1}$ s^{-1} and $k_{NO2} = 8.9\times10^{-12}$ cm^3 $molecule^{-1}$ s^{-1}. The PAN dissociation rate constant, after correcting for the competing PA + NO and PA + NO_2 reactions using Eq. 6, is $5.7(\pm0.8)\times10^{-4}$ s^{-1}, based on three experimental trials. In addition to dissociation, the PAN compound in the 100 L bag could also undergo wall loss. This loss rate was estimated by multiplying the wall loss rate of the ~~carbonyl nitrate~~nitrooxy enal in the 5500 L chamber by a factor of 16, which is the square diffusion distance of the chamber relative to that of the 100 L bag, assuming the PAN compound and the isoprene carbonyl nitrate have similar diffusion and adsorption coefficients. Considering the uncertainty in wall loss rate, the PAN dissociation rate constant is $5.7(+0.8/-2.8)\times10^{-4}$ s^{-1}. Previous studies of the dissociation rate constants for peroxyacyl nitrates have reported results ranging from 1.6×10^{-4} s^{-1} to 6.0×10^{-4} s^{-1} at 298 K (Bridier et al., 1991; Grosjean et al., 1994; Kabir et al., 2014; Roberts and Bertman, 1992). Our result is consistent with previous work.

$$k = k_{PAN}\left(1 - \frac{1}{1+\frac{k_{NO}[NO]}{k_{NO_2}[NO_2]}}\right) \quad \text{(Eq. 6)}$$

Since our OH oxidation experiments were conducted in the presence of high NO concentration, a significant fraction of the PA radicals from the H abstraction reaction channel were expected to react with NO to form alkoxy radicals. Based on the product observed at m/z 321, a reaction scheme (Fig. 11) is proposed, where the alkoxy radical dissociates into CO_2 and an ~~alkyl~~alkenyl radical, which is further oxidized to form a C4 dinitrate (m/z 321, Fig. 10), along with ethanal nitrate (m/z 232, Fig. 10).

For the OH addition pathway, OH can add to the C2 and the C3 position of the ~~4,1 isoprene carbonyl nitrate~~isoprene nitrooxy enal, but the less substituted C3 position should be preferential

(Peeters et al., 2007). For the C2 addition, the expected nitrate products are C5 dinitrate and ethanal nitrate (Fig. 12a), ~~as~~and their nominal masses were observed at m/z 351 and m/z 232 (Fig. 10). NO_2 could potentially be released with the concurrent formation of a C4 di-aldehyde (Fig. 12a). The CIMS signal for this compound at m/z 229 did not increase (Fig. 10), but the CIMS sensitivity for this compound could be relatively low. For the C3 addition, the expected nitrate products are C5 dinitrate, MVK nitrate and ethanal nitrate (Fig. 12b), observed at m/z 351, m/z 276 and m/z 232 (Fig. 10). We assigned m/z 276 to solely MVK nitrate, instead of MACR nitrate, because the precursor nitrooxy enal has a secondary carbon at its C3 position, and the OH oxidation reaction cannot add a functional group at this position while still maintaining it as a secondary carbon as is the case for MACR nitrate. The C2 and C3 OH addition pathway would lead to two C5 dinitrate isomers, but they were detected at the same mass by the CIMS.

Formatted: Font color: Auto

Using a GC-ECD/CIMS method similar to the one described by Xiong et al. (2015), the CIMS sensitivities of the nitrate products were determined relative to the CIMS sensitivity of the ~~4,1-carbonyl nitrate~~isoprene nitrooxy enal. The setup was modified to operate the GC separation under pressure lower than 1 atm (Fig. S7), which helped to lower the elution temperature. A Teflon bag filled with the ~~4,1-carbonyl nitrate~~nitrooxy enal, isopropyl nitrite, and NO was irradiated to generate the OH oxidation products. The mixture of the ~~4,1-carbonyl nitrate~~nitrooxy enal and its products w~~as~~~~ere~~ then cryo-focused and separated on the GC column, and the eluent species were detected by the ECD and the CIMS simultaneously. We were able to quantify the MVK nitrate and the ethanal nitrate using this method, assuming identical ECD sensitivities for nitrates. The other products shown in Fig. 10, however, were not detected with simultaneous good signal-to-noise ratio on the ECD and the CIMS. The ECD/CIMS chromatograms are shown in Fig. 13. We determined that the reaction of the ~~4,1-carbonyl nitrate~~isoprene nitrooxy enal ~~and~~ with the reagent ion I^- could form NO_3^-, but the same reaction did not occur for the MVK nitrate and the ethanal nitrate (Fig. 13). Formation of NO_3^- from I^- reaction with organic nitrates has not been reported previously. Since I^- is a poor nucleophile, it is unclear if this reaction proceeds by S_N2 substitution. Using the same I^- ionization method, Wang et al. (2014) observed NO_3^- signal equivalent to a NO_3 + N_2O_5 concentration of 200-1000 ppt during a field study in Hong Kong. Through interference tests, the authors attributed 30-50% of the observed NO_3^- signal to the interference from peroxyacetyl nitrate and NO_2. Since I^- reaction with the ~~carbonyl nitrate~~nitrooxy enal can also generate NO_3^-, organic nitrates ($RONO_2$) could be a potential source of interference for NO_3 +

N_2O_5 measurement with the I^- ionization method. For field measurement of isoprene nitrooxy enal, this compound could be mistakenly measured as NO_3^- when iodide-based CIMS was used without tuning the instrument specifically to favor iodide-nitrate clustering. While no field observations of this type of compound have been reported to date, they can still potentially be an important NO_y reservoir. For instance, Brown et al. (2009) estimated that in the 2004 NEAQS study the total concentration of nitrates derived from NO_3 + isoprene chemistry could reach 500 ppt. The carbonyl nitrates (nitrooxy enone and nitrooxy enal) can contribute to a significant fraction of the total.

For the GC-ECD/CIMS calibration, 9 trials were conducted at three different pressures. The results are summarized in Table S2. The relative CIMS sensitivities for the nitrooxy enal~~4,1 carbonyl nitrate~~, ethanal nitrate and MVK nitrate are 1:15(±3):34(±3) respectively. The absolute CIMS sensitivity of the ~~4,1 carbonyl nitrate~~isoprene nitrooxy enal was determined with standard gas samples prepared following Xiong et al. (2015), and the result was used to calculate the absolute sensitivities for the ethanal nitrate and the MVK nitrate. The ethanal nitrate and the MVK nitrate both have the $–ONO_2$ group at the β position of the acidic H, so their CIMS sensitivities are comparable. For the MVK nitrate, the electron-withdrawing ketone group can further enhance its gas-phase acidity and its affinity to bind with I^-. Hence, the CIMS sensitivity for the MVK nitrate is greater than for the ethanal nitrate. For the ~~4,1 carbonyl nitrate~~nitrooxy enal, its low CIMS sensitivity can be caused by the *trans*-δ configuration of the $–ONO_2$ group and the –CHO group. Our previous studies on isoprene-derived hydroxynitrates suggested that the CIMS sensitivity for the β isomer is 8 times greater than for the *trans*-δ isomer (Xiong et al., 2015). Lee et al. (2014a) also reported the β isomer sensitivity being over 16 times greater than the *trans*-δ isomer sensitivity, using iodide as the reagent ion. Hence, our calibration results, with the sensitivity for the ethanal nitrate 15 times greater than the sensitivity for the ~~4,1 carbonyl nitrate~~nitrooxy enal, is consistent with previous work.

With the CIMS sensitivities determined, the yield of the MVK nitrate and the ethanal nitrate from the OH-initiated oxidation of ~~4,1 carbonyl nitrate~~the isoprene nitrooxy enal was obtained by comparing the formation of the products relative to the loss of the reactant (Fig. 14). The yield of the ethanal nitrate was corrected for loss to OH oxidation and photolysis, using the method described by Tuazon et al. (1984). The applied ethanal nitrate + OH rate constant was 3.4×10^{-12} cm^3 $molecules^{-1}$ s^{-1}, calculated using the structure-reactivity relationship (SAR) proposed by

Formatted: Font color: Auto

Formatted: Font color: Auto

Formatted: Font color: Auto

Kwok and Atkinson (1995). The applied photolysis frequency for ethanal nitrate was 1.69×10^{-5} s^{-1}, calculated with the cross section recommended by Muller el al (2014) and a unity quantum yield. ~~The photolysis frequency of the isoprene carbonyl nitrate was applied to account for the photolytic loss of ethanal nitrate inside the chamber, because the β ketone group is known to enhance the absorption cross section of the nitrate (Müller et al., 2014).~~The yield of the MVK nitrate was corrected for loss to photolysis, wall uptake and OH oxidation using the same method as that for the ethanal nitrate yield. ~~For the MVK nitrate, no OH loss correction was applied, because MVK nitrate is saturated and is not expected to undergo significant loss to OH~~The applied photolysis frequency for the MVK nitrate was 4.5×10^{-6} s^{-1}, calculated using the absorption cross section of 3-nitrooxy-2-butanone (Barnes et al., 1993) as a surrogate and unity quantum yield across all wavelengths (Müller et al., 2014). ~~However, its loss to wall uptake and photolysis loss was corrected, following the same method as used for the ethanal nitrate.~~ The MVK nitrate ~~loss rates~~wall loss rate ~~for wall uptake and photolysis inside the chamber were~~ was set the same as ~~those~~ that for the ~~4,1 carbonyl nitrate~~nitrooxy enal, because MVK nitrate ~~is also a ketone nitrate, which is prone to photolysis loss, and it~~ has a molecular weight close to that of the nitrooxy enal~~4,1 carbonyl nitrate~~. Based on the Kwok and Atkinson (1995) SAR method, we calculated that the rate constant for MVK nitrate reaction with OH should be 1.78×10^{-12} cm^3 $molecules^{-1}$ s^{-1}. After the correction for secondary loss, ~~T~~the apparent yield is ~~24.5~~23.3% for MVK nitrate and ~~8.08~~8.0% for ethanal nitrate. Considering the uncertainties in the sensitivities of MVK nitrate and ethanal nitrate (Table S2), the MVK nitrate yield is ~~24~~23(±3)%, and the ethanal nitrate yield is 8(±2)%. The fractional inlet sampling loss for the three nitrates was determined by comparing the CIMS signals of sampling through the 5.2 m long 50°C tubing and through a 20 cm room temperature tubing. By correcting for the inlet sampling loss, the MVK nitrate yield is ~~24~~23(±5)%, and the ethanal nitrate yield is 8(±3)%. For the two OH oxidation experiments, the first-order loss rate of the ~~4,1 carbonyl nitrate~~nitrooxy enal was 3×10^{-4} s^{-1} (Fig. S8). Since the total wall uptake and photolysis loss rate for ~~4,1 isoprene carbonyl nitrate~~nitrooxy enal was 4.3×10^{-5} s^{-1}, approximately 85% of the ~~4,1 carbonyl nitrate~~nitrooxy enal was lost to OH oxidation. After correcting for this factor, the MVK nitrate yield is ~~28~~27(±5)%, and the ethanal nitrate yield is 9(±3)%. While we were able to determine the yields of MVK nitrate and ethanal nitrate from the OH oxidation reaction, the exact branching ratios for reactions described in Fig. 11 and 12 cannot be derived. This is because ethanal nitrate can be produced in both H abstraction and OH addition pathways (including both the (a)

Formatted: Font color: Auto

Formatted: Font color: Auto

Formatted: Font color: Auto

Formatted: Font color: Auto

Formatted: Font color: Auto

and (b) pathways). For MVK nitrate, even though it is produced in pathway (b) only, it has ethanal nitrate as a byproduct, making it impossible for us to determine the branching ratio for pathway (b).

4.3.2 Photolysis

Previous work on acetaldehyde suggests that at 313 nm the dominant photolysis reaction is dissociation of the C−CHO bond, forming a formyl radical (•CHO) (Blacet and Loeffler, 1942). At shorter wavelength (265 nm), the reaction can proceed by intramolecular rearrangement forming CH_4 and CO (Blacet and Loeffler, 1942). For compounds with longer carbon chain length, such as propyl- and butyl- aldehydes, the photo-dissociation reaction can produce alkenes and smaller aldehydes at 238 nm and 187 nm (Blacet and Crane, 1954). Since the UV radiation that reaches the earth's surface is mostly above 300 nm, the formyl radical pathway is expected to be the most important photolysis reaction for alkyl aldehydes (Shepson and Heicklen, 1982). For the isoprene ~~carbonyl nitrate~~nitrooxy enal, the C−CHO bond is strengthened by the delocalized electrons from the vinyl and the carbonyl groups, leading to a bond dissociation energy of 413 kJ/mol, as measured for acrolein, which is larger than the C−CHO bond dissociation energy of acetaldehyde (355 kJ/mol) (Wiberg et al., 1992). In comparison, the O−NO_2 bond dissociation energy is 175 kJ/mol (Luo, 2007a), much lower than the dissociation energy of the C−CHO bond. Hence, dissociation of the weak O−NO_2 bond may be an important reaction pathway for the ~~carbonyl nitrate~~nitrooxy enal. This process likely involves the absorption of a photon by the C=C−C=O chromophore, followed by intramolecular energy redistribution to deposit energy into the O−NO_2 bond prior to dissociation. This reaction step would generate NO_2 and an alkoxy radical, which upon reaction with O_2 forms a conjugated dialdehyde.

Fig. 15 shows the CIMS spectra before and after the photolysis of the isoprene ~~carbonyl nitrate~~nitrooxy enal. Cyclohexane was used as the OH scavenger for this experiment. The CIMS signal for the dialdehyde, which is the O−NO_2 bond dissociation product (reaction mechanism shown in Fig. 16), did not increase significantly. This may be because the CIMS was not sensitive to the dialdehyde, and/or the dialdehyde underwent rapid secondary reactions, rendering its steady-state concentration below the CIMS detection limit. Alternatively, it is possible that the alkoxy radical derived from O−NO_2 bond dissociation undergoes a 1,5-H shift reaction (Fig. 16), rendering the formation of the dialdehyde an insignificant pathway. The resulting alkyl radical can

immediately form a peroxy radical, which may follow the H shift mechanism proposed by Peeters et al. (2009) and form a hydroperoxy aldehyde (HPALD) compound, as observed at m/z 257 by the CIMS (Fig. 15). When the peroxy radical reacts with NO or RO_2, the resulting alkoxy radical will form a hydroxy dialdehyde (Fig. 16) with m/z ratio at 241, which was also observed by the CIMS (Fig. 14). It is worth noting that we also observed CIMS signals for the deprotonated ions derived from the HPALD compound (m/z 129 and m/z 147) and the hydroxy dialdehyde (m/z 113 and m/z 131). The proton transfer reaction between the iodide ion and alcohols/peroxides have not been observed previously, but it is possible that the conjugated structures help stabilize the charge and hence make the proton transfer reaction a viable reaction channel.

The product at m/z 276 has the molecular weight of MVK nitrate. In the presence of OH scavenger, however, the reaction is unlikely to proceed by the OH-initiated oxidation pathway to form MVK nitrate. Instead, we hypothesize that the isoprene ~~carbonyl nitrate~~nitrooxy enal could dissociate via the C−CHO bond, which, following reaction with O_2 and HO_2, would form a vinyl hydroperoxide with the same molecular weight as MVK nitrate. Vinyl hydroperoxides are known to be a reactive intermediate from the intramolecular H shift of Criegee biradical, which can decompose into OH and alkoxy radicals (Kroll et al., 2002). However, the un-energized vinyl hydroperoxides should have a lifetime long enough to be detected by mass spectrometers (Liu et al., 2015). In fact, theoretical calculations suggest that at 25 °C vinyl hydroperoxide has a lifetime of 58 hours (Richardson, 1995). Therefore, the product at m/z 276 is likely the vinyl hydroperoxide. For the OH oxidation product experiments, however, we attributed m/z 276 to MVK nitrate only, because RO_2 + NO reaction (forming MVK nitrate) should dominate over RO_2 + HO_2 reaction (forming vinyl hydroperoxide), in the presence of high NO concentration.

Based on the CIMS spectra of the photolysis products, we conclude that the photolysis of the isoprene ~~carbonyl nitrate~~nitrooxy enal leads to the dissociation of both the O−NO_2 and the C−CHO bonds. A reaction scheme is proposed in Fig. 16. While we were able to identify some of the photolysis products based on the nominal masses observed with the CIMS, the branching ratio for the two reaction pathways was not determined, due to lack of quantitative measurements during the photolysis experiment. Future studies are needed to evaluate the relative importance of these two processes.

5 Conclusions and future work

An isoprene-derived ~~carbonyl nitrate~~nitrooxy enal model compound was synthesized to study its photochemical degradation chemistry in the atmosphere. The UV absorption spectrum of this compound has contributions from both the C=C−C=O and the $–ONO_2$ chromophores, as is confirmed by theoretical calculations, but absorption in the actinic region involves a transition involving the enal~~carbonyl~~ group. The combination of the C=C−C=O and the $–ONO_2$ chromophores enhances the UV cross section of this molecule relative to alkyl nitrates, making photolysis its dominant daytime sink. The photochemical lifetime of the ~~carbonyl nitrate~~nitrooxy enal can be less than one hour, due to its rapid photolysis loss, together with high reactivity toward OH and O_3. The OH and O_3 oxidation rate constants for the ~~4,1-~~isoprene ~~carbonyl nitrate~~nitrooxy enal obtained in this study were both smaller than the reported rate constants for the δ-isoprene hydroxy nitrates (Jacobs et al., 2014; Lee et al., 2014b). This could be because the oxidation by either OH or O_3 would break the resonance structure of the C=C−C=O moiety, thus increasing the activation energy.

Using the iodide-based CIMS, we identified the first-generation nitrate products from the OH-initiated oxidation of the synthesized ~~carbonyl nitrate~~nitrooxy enal, including mononitrate, dinitrate and nitrooxy peroxyacyl nitrate. Two of the products, the MVK nitrate and the ethanal nitrate, were quantified, which together contributed to ~~37~~36(±5)% of the total products. The CIMS spectra of the nitrate photolysis products suggest that both the C−CHO bond and the $O–NO_2$ bond dissociate in the reaction. Since photolysis is a significant sink for the ~~carbonyl nitrate~~nitrooxy enal, it is important for future studies to investigate the relative importance of the two reaction pathways, in order to fully understand the fate of NO_x in isoprene-rich atmospheres. Dissociation of the $O–NO_2$ bond may afford highly oxidized alcohol and hydroperoxide, which can potentially undergo uptake into the particle phase and facilitate the formation of secondary organic aerosols. The C−CHO dissociation pathway may form a vinyl hydroperoxide product.

The NO_3-initiated isoprene oxidation can produce a series of isomeric carbonyl nitrates. The 1,4-~~carbonyl~~ nitrooxy enal~~nitrate~~, which is the dominant isomer, is expected to have similar photolysis reactivity as the 4,1-~~carbonyl nitrate~~nitrooxy enal studied in this work, because they both have the O=C−C=C−C chromophore and the $−ONO_2$ chromophore, which would enhance the molecular

absorption cross section. For the unsaturated ketones (enones) derived from isoprene oxidation, the ketone functionality may reduce their reactivity toward OH, in comparison with aldehydes, but we expect them to have similar photochemical properties as the nitrooxy enals, since isomers such as methyl vinyl ketone (MVK) and methacrolein (MACR) have similar absorption cross sections and quantum yields (Gierczak et al., 1997).

~~The influence of the unsaturated ketone functionality on nitrate photolysis is still unclear, and future studies are needed to understand how the different conjugated structures can affect the photochemical processes.~~

The experiments in this work were conducted in the presence of relatively high NO concentration. In the ambient environment, organic nitrates produced in the high NO_x regime can undergo photochemical degradation in the low NO regime, due to the wide span of ambient NO_x concentrations (Su et al., 2015; Xiong et al., 2015). Crounse et al. (2012) proposed that under low NO conditions, the oxidation of methacrolein (MACR) can regenerate OH radicals and form a lactone that is prone to reactive uptake onto the aerosol phase. Since the ~~4,1 carbonyl nitrate~~isoprene nitrooxy enal has a structure similar to that of MACR, it might also undergo similar reaction in the clean environment. Further experimental work is needed to investigate how the photochemical oxidation process of the ~~carbonyl nitrate~~nitrooxy enal can influence the formation of OH radicals and growth of secondary organic aerosols.

Acknowledgement

This research was supported in part through computational resources provided by Information Technology at Purdue University. We thank the National Science Foundation for supporting CHB and LVS (grant CHE-1465154), and FX and PBS (grant AGS-1228496).

References

Aschmann, S. M., Tuazon, E. C., Arey, J., and Atkinson, R.: Products of the OH radical-initiated reactions of 2-propyl nitrate, 3-methyl-2-butyl nitrate and 3-methyl-2-pentyl nitrate, Atmospheric Environment, 45, 1695-1701, http://dx.doi.org/10.1016/j.atmosenv.2010.12.061, 2011.

611 Atkinson, R., and Aschmann, S. M.: Kinetics of the gas phase reaction of Cl atoms with a series of
612 organics at 296 ± 2 K and atmospheric pressure, International Journal of Chemical Kinetics, 17,
613 33-41, 10.1002/kin.550170105, 1985.

614 Atkinson, R., Baulch, D. L., Cox, R. A., Crowley, J. N., Hampson, R. F., Hynes, R. G., Jenkin, M. E.,
615 Rossi, M. J., and Troe, J.: Evaluated kinetic and photochemical data for atmospheric chemistry:
616 Volume III – gas phase reactions of inorganic halogens, Atmos. Chem. Phys., 7, 981-1191,
617 10.5194/acp-7-981-2007, 2007.

618 Barnes, I., Becker, K. H., and Zhu, T.: Near UV absorption spectra and photolysis products of
619 difunctional organic nitrates: Possible importance as NO x reservoirs, Journal of Atmospheric
620 Chemistry, 17, 353-373, 10.1007/bf00696854, 1993.

621 Bayliss, N. S., and McRae, E. G.: Solvent Effects in the Spectra of Acetone, Crotonaldehyde,
622 Nitromethane and Nitrobenzene, The Journal of Physical Chemistry, 58, 1006-1011,
623 10.1021/j150521a018, 1954.

624 Blacet, F. E., and Loeffler, D. E.: The Photolysis of the Aliphatic Aldehydes. XI. Acetaldehyde and
625 Iodine Mixtures, Journal of the American Chemical Society, 64, 893-896, 10.1021/ja01256a045,
626 1942.

627 Blacet, F. E.: Photochemistry in the Lower Atmosphere, Industrial & Engineering Chemistry, 44,
628 1339-1342, 10.1021/ie50510a044, 1952.

629 Blacet, F. E., and Crane, R. A.: The Photolysis of the Aliphatic Aldehydes. XVII. Propionaldehyde,
630 n-Butyraldehyde and Isobutyraldehyde at 2380 and 1870 Å, Journal of the American Chemical
631 Society, 76, 5337-5340, 10.1021/ja01650a020, 1954.

632 Braun, W., Fahr, A., Klein, R., Kurylo, M. J., and Huie, R. E.: UV gas and liquid phase absorption
633 cross section measurements of hydrochlorofluorocarbons HCFC-225ca and HCFC-225cb, Journal
634 of Geophysical Research: Atmospheres, 96, 13009-13015, 10.1029/91JD01026, 1991.

635 Bridier, I., Caralp, F., Loirat, H., Lesclaux, R., Veyret, B., Becker, K. H., Reimer, A., and Zabel, F.:
636 Kinetic and theoretical studies of the reactions acetylperoxy + nitrogen dioxide + M .dblarw.
637 acetyl peroxynitrate + M between 248 and 393 K and between 30 and 760 torr, The Journal of
638 Physical Chemistry, 95, 3594-3600, 10.1021/j100162a031, 1991.

639 Brown, S. S., deGouw, J. A., Warneke, C., Ryerson, T. B., Dubé, W. P., Atlas, E., Weber, R. J., Peltier,
640 R. E., Neuman, J. A., Roberts, J. M., Swanson, A., Flocke, F., McKeen, S. A., Brioude, J., Sommariva,
641 R., Trainer, M., Fehsenfeld, F. C., and Ravishankara, A. R.: Nocturnal isoprene oxidation over the
642 Northeast United States in summer and its impact on reactive nitrogen partitioning and
643 secondary organic aerosol, Atmos. Chem. Phys., 9, 3027-3042, 10.5194/acp-9-3027-2009, 2009.

644 Chai, J.-D., and Head-Gordon, M.: Long-range corrected hybrid density functionals with damped
645 atom-atom dispersion corrections, Physical Chemistry Chemical Physics, 10, 6615-6620,
646 10.1039/B810189B, 2008.

647 Chameides, W., and Walker, J. C. G.: A photochemical theory of tropospheric ozone, Journal of
648 Geophysical Research, 78, 8751-8760, 10.1029/JC078i036p08751, 1973.

649 Chameides, W., Lindsay, R., Richardson, J., and Kiang, C.: The role of biogenic hydrocarbons in
650 urban photochemical smog: Atlanta as a case study, Science, 241, 1473-1475,
651 10.1126/science.3420404, 1988.

652 Chameides, W. L., Fehsenfeld, F., Rodgers, M. O., Cardelino, C., Martinez, J., Parrish, D.,
653 Lonneman, W., Lawson, D. R., Rasmussen, R. A., Zimmerman, P., Greenberg, J., Mlddleton, P.,
654 and Wang, T.: Ozone precursor relationships in the ambient atmosphere, Journal of Geophysical
655 Research: Atmospheres, 97, 6037-6055, 10.1029/91JD03014, 1992.

656 Chen, X., Hulbert, D., and Shepson, P. B.: Measurement of the organic nitrate yield from OH
657 reaction with isoprene, Journal of Geophysical Research, 103, 25563, 10.1029/98jd01483, 1998.

658 Crounse, J. D., Knap, H. C., Ornso, K. B., Jorgensen, S., Paulot, F., Kjaergaard, H. G., and Wennberg,
659 P. O.: Atmospheric fate of methacrolein. 1. Peroxy radical isomerization following addition of OH
660 and O2, The journal of physical chemistry. A, 116, 5756-5762, 10.1021/jp211560u, 2012.

661 Darer, A. I., Cole-Filipiak, N. C., O'Connor, A. E., and Elrod, M. J.: Formation and stability of
662 atmospherically relevant isoprene-derived organosulfates and organonitrates, Environmental
663 science & technology, 45, 1895-1902, 10.1021/es103797z, 2011.

664 Ferris, A. F., McLean, K. W., Marks, I. G., and Emmons, W. D.: Metathetical Reactions of Silver
665 Salts in Solution. III. The Synthesis of Nitrate Esters1, Journal of the American Chemical Society,
666 75, 4078-4078, 10.1021/ja01112a505, 1953.

667 Frisch, M. J., Pople, J. A., and Binkley, J. S.: Self‐consistent molecular orbital methods 25.
668 Supplementary functions for Gaussian basis sets, The Journal of Chemical Physics, 80, 3265-3269,
669 doi:http://dx.doi.org/10.1063/1.447079, 1984.

670 Giacopelli, P., Ford, K., Espada, C., and Shepson, P. B.: Comparison of the measured and simulated
671 isoprene nitrate distributions above a forest canopy, Journal of Geophysical Research, 110,
672 D01304, 10.1029/2004jd005123, 2005.

673 Gierczak, T., Burkholder, J. B., Talukdar, R. K., Mellouki, A., Barone, S. B., and Ravishankara, A. R.:
674 Atmospheric fate of methyl vinyl ketone and methacrolein, Journal of Photochemistry and
675 Photobiology A: Chemistry, 110, 1-10, http://dx.doi.org/10.1016/S1010-6030(97)00159-7, 1997.

676 Gilbert, A. T. B.: IQmol molecular viewer, 2012.

677 Gray, G. M.: Method for the preparation of (E)-4-bromo-2-methylbut-2-en-1-al 4288635, 1981.

678 Grosjean, D., Grosjean, E., and Williams, E. L.: Thermal decomposition of C3-substituted
679 peroxyacyl nitrates, Res Chem Intermed, 20, 447-461, 10.1163/156856794X00414, 1994.

Grossenbacher, J. W., Barket Jr, D. J., Shepson, P. B., Carroll, M. A., Olszyna, K., and Apel, E.: A comparison of isoprene nitrate concentrations at two forest-impacted sites, Journal of Geophysical Research: Atmospheres, 109, D11311, 10.1029/2003JD003966, 2004.

Haagen-Smit, A. J.: Chemistry and Physiology of Los Angeles Smog, Industrial & Engineering Chemistry, 44, 1342-1346, 10.1021/ie50510a045, 1952.

Hallquist, M., WÄngberg, I., and LjungstrÖm, E.: Atmospheric Fate of Carbonyl Oxidation Products Originating from α-Pinene and Δ3-Carene: Determination of Rate of Reaction with OH and NO3 Radicals, UV Absorption Cross Sections, and Vapor Pressures, Environmental science & technology, 31, 3166-3172, 10.1021/es970151a, 1997.

Hens, K., Novelli, A., Martinez, M., Auld, J., Axinte, R., Bohn, B., Fischer, H., Keronen, P., Kubistin, D., Nölscher, A. C., Oswald, R., Paasonen, P., Petäjä, T., Regelin, E., Sander, R., Sinha, V., Sipilä, M., Taraborrelli, D., Tatum Ernest, C., Williams, J., Lelieveld, J., and Harder, H.: Observation and modelling of HO2 radicals in a boreal forest, Atmospheric Chemistry and Physics, 14, 8723-8747, 10.5194/acp-14-8723-2014, 2014.

Herron, J. T., and Huie, R. E.: Rate constants for the reactions of ozone with ethene and propene, from 235.0 to 362.0.deg.K, The Journal of Physical Chemistry, 78, 2085-2088, 10.1021/j100614a004, 1974.

Hohenberg, P., and Kohn, W.: Inhomogeneous Electron Gas, Physical Review, 136, B864-B871, 1964.

Horowitz, L. W., Fiore, A. M., Milly, G. P., Cohen, R. C., Perring, A., Wooldridge, P. J., Hess, P. G., Emmons, L. K., and Lamarque, J.-F.: Observational constraints on the chemistry of isoprene nitrates over the eastern United States, Journal of Geophysical Research, 112, D12S08, 10.1029/2006jd007747, 2007.

Hu, K. S., Darer, A. I., and Elrod, M. J.: Thermodynamics and kinetics of the hydrolysis of atmospherically relevant organonitrates and organosulfates, Atmospheric Chemistry and Physics, 11, 8307-8320, 10.5194/acp-11-8307-2011, 2011.

Jacobs, M. I., Burke, W. J., and Elrod, M. J.: Kinetics of the reactions of isoprene-derived hydroxynitrates: gas phase epoxide formation and solution phase hydrolysis, Atmospheric Chemistry and Physics, 14, 8933-8946, 10.5194/acp-14-8933-2014, 2014.

Kabir, M., Jagiella, S., and Zabel, F.: Thermal Stability of n-Acyl Peroxynitrates, International Journal of Chemical Kinetics, 46, 462-469, 10.1002/kin.20862, 2014.

Klein, T., Barnes, I., Becker, K. H., Fink, E. H., and Zabel, F.: Pressure dependence of the rate constants for the reactions of ethene and propene with hydroxyl radicals at 295 K, The Journal of Physical Chemistry, 88, 5020-5025, 10.1021/j150665a046, 1984.

714 Kohn, W., and Sham, L. J.: Self-Consistent Equations Including Exchange and Correlation Effects,
715 Physical Review, 140, A1133-A1138, 1965.

716 Kroll, J. H., Donahue, N. M., Cee, V. J., Demerjian, K. L., and Anderson, J. G.: Gas-Phase Ozonolysis
717 of Alkenes: Formation of OH from Anti Carbonyl Oxides, Journal of the American Chemical
718 Society, 124, 8518-8519, 10.1021/ja0266060, 2002.

719 Kwan, A. J., Chan, A. W. H., Ng, N. L., Kjaergaard, H. G., Seinfeld, J. H., and Wennberg, P. O.: Peroxy
720 radical chemistry and OH radical production during the NO₃-initiated oxidation of
721 isoprene, Atmospheric Chemistry and Physics, 12, 7499-7515, 10.5194/acp-12-7499-2012, 2012.

722 Kwok, E. S. C., and Atkinson, R.: Estimation of hydroxyl radical reaction rate constants for gas-
723 phase organic compounds using a structure-reactivity relationship: An update, Atmospheric
724 Environment, 29, 1685-1695, http://dx.doi.org/10.1016/1352-2310(95)00069-B, 1995.

725 Lee, B. H., Lopez-Hilfiker, F. D., Mohr, C., Kurtén, T., Worsnop, D. R., and Thornton, J. A.: An Iodide-
726 Adduct High-Resolution Time-of-Flight Chemical-Ionization Mass Spectrometer: Application to
727 Atmospheric Inorganic and Organic Compounds, Environmental science & technology, 48, 6309-
728 6317, 10.1021/es500362a, 2014a.

729 Lee, L., Teng, A. P., Wennberg, P. O., Crounse, J. D., and Cohen, R. C.: On rates and mechanisms
730 of OH and O3 reactions with isoprene-derived hydroxy nitrates, The journal of physical chemistry.
731 A, 118, 1622-1637, 10.1021/jp4107603, 2014b.

732 Lefohn, A. S., and Foley, J. K.: Establishing Relevant Ozone Standards to Protect Vegetation and
733 Human Health: Exposure/Dose-Response Considerations, Air & Waste, 43, 106-112,
734 10.1080/1073161X.1993.10467111, 1993.

735 Linder, B., and Abdulnur, S.: Solvent Effects on Electronic Spectral Intensities, The Journal of
736 Chemical Physics, 54, 1807-1814, doi:http://dx.doi.org/10.1063/1.1675088, 1971.

737 Lippmann, M.: HEALTH EFFECTS OF OZONE A Critical Review, JAPCA, 39, 672-695,
738 10.1080/08940630.1989.10466554, 1989.

739 Liu, F., Fang, Y., Kumar, M., Thompson, W. H., and Lester, M. I.: Direct observation of vinyl
740 hydroperoxide, Physical Chemistry Chemical Physics, 17, 20490-20494, 10.1039/C5CP02917A,
741 2015.

742 Lockwood, A. L., Shepson, P. B., Fiddler, M. N., and Alaghmand, M.: Isoprene nitrates: preparation,
743 separation, identification, yields, and atmospheric chemistry, Atmospheric Chemistry and Physics,
744 10, 6169-6178, 10.5194/acp-10-6169-2010, 2010.

745 Lu, K. D., Rohrer, F., Holland, F., Fuchs, H., Bohn, B., Brauers, T., Chang, C. C., Häseler, R., Hu, M.,
746 Kita, K., Kondo, Y., Li, X., Lou, S. R., Nehr, S., Shao, M., Zeng, L. M., Wahner, A., Zhang, Y. H., and
747 Hofzumahaus, A.: Observation and modelling of OH and HO2 concentrations in the Pearl River

748 Delta 2006: a missing OH source in a VOC rich atmosphere, Atmos. Chem. Phys., 12, 1541-1569,
749 10.5194/acp-12-1541-2012, 2012.

750 Luo, Y.-R.: BDEs of O-X bonds, in: Comprehensive Handbook of Chemical Bond Energies, CRC Press,
751 351, 2007a.

752 Luo, Y.-R.: BDEs in the halogenated molecules, clusters and complexes, in: Comprehensive
753 Handbook of Chemical Bond Energies, CRC Press, 1351-1427, 2007b.

754 Madronich, S., and Flocke, S.: The role of solar radiation in atmospheric chemistry, in: Handbook
755 of Environmental Chemistry, edited by: Boule, P., Springer-Verlag, Heidelberg, 1-26, 1998.

756 Mao, J., Paulot, F., Jacob, D. J., Cohen, R. C., Crounse, J. D., Wennberg, P. O., Keller, C. A., Hudman,
757 R. C., Barkley, M. P., and Horowitz, L. W.: Ozone and organic nitrates over the eastern United
758 States: Sensitivity to isoprene chemistry, Journal of Geophysical Research: Atmospheres, 118,
759 11,256-211,268, 10.1002/jgrd.50817, 2013.

760 Martinez, M., Harder, H., Kovacs, T. A., Simpas, J. B., Bassis, J., Lesher, R., Brune, W. H., Frost, G.
761 J., Williams, E. J., Stroud, C. A., Jobson, B. T., Roberts, J. M., Hall, S. R., Shetter, R. E., Wert, B.,
762 Fried, A., Alicke, B., Stutz, J., Young, V. L., White, A. B., and Zamora, R. J.: OH and HO2
763 concentrations, sources, and loss rates during the Southern Oxidants Study in Nashville,
764 Tennessee, summer 1999, Journal of Geophysical Research: Atmospheres, 108, n/a-n/a,
765 10.1029/2003JD003551, 2003.

766 Mihelcic, D., Holland, F., Hofzumahaus, A., Hoppe, L., Konrad, S., Müsgen, P., Pätz, H. W., Schäfer,
767 H. J., Schmitz, T., Volz-Thomas, A., Bächmann, K., Schlomski, S., Platt, U., Geyer, A., Alicke, B., and
768 Moortgat, G. K.: Peroxy radicals during BERLIOZ at Pabstthum: Measurements, radical budgets
769 and ozone production, Journal of Geophysical Research: Atmospheres, 108, n/a-n/a,
770 10.1029/2001JD001014, 2003.

771 Müller, J. F., Peeters, J., and Stavrakou, T.: Fast photolysis of carbonyl nitrates from isoprene,
772 Atmospheric Chemistry and Physics, 14, 2497-2508, 10.5194/acp-14-2497-2014, 2014.

773 Neuman, J. A., Nowak, J. B., Huey, L. G., Burkholder, J. B., Dibb, J. E., Holloway, J. S., Liao, J., Peischl,
774 J., Roberts, J. M., Ryerson, T. B., Scheuer, E., Stark, H., Stickel, R. E., Tanner, D. J., and Weinheimer,
775 A.: Bromine measurements in ozone depleted air over the Arctic Ocean, Atmos. Chem. Phys., 10,
776 6503-6514, 10.5194/acp-10-6503-2010, 2010.

777 Noyes, W. A.: Explanation of the Formation of Alkyl Nitrites in Dilute Solutions; Butyl and Amyl
778 Nitrites, Journal of the American Chemical Society, 55, 3888-3889, 10.1021/ja01336a503, 1933.

779 Parrish, D. D., Lamarque, J. F., Naik, V., Horowitz, L., Shindell, D. T., Staehelin, J., Derwent, R.,
780 Cooper, O. R., Tanimoto, H., Volz-Thomas, A., Gilge, S., Scheel, H. E., Steinbacher, M., and Fröhlich,
781 M.: Long-term changes in lower tropospheric baseline ozone concentrations: Comparing
782 chemistry-climate models and observations at northern midlatitudes, Journal of Geophysical
783 Research: Atmospheres, 119, 5719-5736, 10.1002/2013JD021435, 2014.

784 Patchen, A. K., Pennino, M. J., Kiep, A. C., and Elrod, M. J.: Direct kinetics study of the product-
785 forming channels of the reaction of isoprene-derived hydroxyperoxy radicals with NO,
786 International Journal of Chemical Kinetics, 39, 353-361, 10.1002/kin.20248, 2007.

787 Paulot, F., Crounse, J. D., Kjaergaard, H. G., Kroll, J. H., Seinfeld, J. H., and Wennberg, P. O.:
788 Isoprene photooxidation: new insights into the production of acids and organic nitrates, Atmos.
789 Chem. Phys., 9, 1479-1501, 10.5194/acp-9-1479-2009, 2009.

790 Paulot, F., Henze, D. K., and Wennberg, P. O.: Impact of the isoprene photochemical cascade on
791 tropical ozone, Atmospheric Chemistry and Physics, 12, 1307-1325, 10.5194/acp-12-1307-2012,
792 2012.

793 Peeters, J., Boullart, W., Pultau, V., Vandenberk, S., and Vereecken, L.: Structure−Activity
794 Relationship for the Addition of OH to (Poly)alkenes: Site-Specific and Total Rate Constants, The
795 Journal of Physical Chemistry A, 111, 1618-1631, 10.1021/jp066973o, 2007.

796 Peeters, J., Nguyen, T. L., and Vereecken, L.: HOx radical regeneration in the oxidation of isoprene,
797 Physical chemistry chemical physics : PCCP, 11, 5935-5939, 10.1039/b908511d, 2009.

798 Perring, A. E., Wisthaler, A., Graus, M., Wooldridge, P. J., Lockwood, A. L., Mielke, L. H., Shepson,
799 P. B., Hansel, A., and Cohen, R. C.: A product study of the isoprene+NO3 reaction, Atmos. Chem.
800 Phys., 9, 4945-4956, 10.5194/acp-9-4945-2009, 2009.

801 Platt, U., Alicke, B., Dubois, R., Geyer, A., Hofzumahaus, A., Holland, F., Martinez, M., Mihelcic,
802 D., Klüpfel, T., Lohrmann, B., Pätz, W., Perner, D., Rohrer, F., Schäfer, J., and Stutz, J.: Free Radicals
803 and Fast Photochemistry during BERLIOZ, Journal of Atmospheric Chemistry, 42, 359-394,
804 10.1023/A:1015707531660, 2002.

805 Richardson, W. H.: An Evaluation of Vinyl Hydroperoxide as an Isolable Molecule, The Journal of
806 Organic Chemistry, 60, 4090-4095, 10.1021/jo00118a027, 1995.

807 Rindelaub, J. D., McAvey, K. M., and Shepson, P. B.: The photochemical production of organic
808 nitrates from α-pinene and loss via acid-dependent particle phase hydrolysis, Atmospheric
809 Environment, 100, 193-201, http://dx.doi.org/10.1016/j.atmosenv.2014.11.010, 2015.

810 Roberts, J. M.: The atmospheric chemistry of organic nitrates, Atmospheric Environment. Part A.
811 General Topics, 24, 243-287, http://dx.doi.org/10.1016/0960-1686(90)90108-Y, 1990.

812 Roberts, J. M., and Bertman, S. B.: The thermal decomposition of peroxyacetic nitric anhydride
813 (PAN) and peroxymethacrylic nitric anhydride (MPAN), International Journal of Chemical Kinetics,
814 24, 297-307, 10.1002/kin.550240307, 1992.

815 Roberts, J. M., Flocke, F., Stroud, C. A., Hereid, D., Williams, E., Fehsenfeld, F., Brune, W., Martinez,
816 M., and Harder, H.: Ground-based measurements of peroxycarboxylic nitric anhydrides (PANs)
817 during the 1999 Southern Oxidants Study Nashville Intensive, Journal of Geophysical Research:
818 Atmospheres, 107, ACH 1-1-ACH 1-10, 10.1029/2001JD000947, 2002.

819 Rollins, A. W., Kiendler-Scharr, A., Fry, J. L., Brauers, T., Brown, S. S., Dorn, H. P., Dubé, W. P.,
820 Fuchs, H., Mensah, A., Mentel, T. F., Rohrer, F., Tillmann, R., Wegener, R., Wooldridge, P. J., and
821 Cohen, R. C.: Isoprene oxidation by nitrate radical: alkyl nitrate and secondary organic aerosol
822 yields, Atmos. Chem. Phys., 9, 6685-6703, 10.5194/acp-9-6685-2009, 2009.

823 Runge, E., and Gross, E. K. U.: Density-Functional Theory for Time-Dependent Systems, Physical
824 Review Letters, 52, 997-1000, 1984.

825 Schwantes, R. H., Teng, A. P., Nguyen, T. B., Coggon, M. M., Crounse, J. D., St. Clair, J. M., Zhang,
826 X., Schilling, K. A., Seinfeld, J. H., and Wennberg, P. O.: Isoprene NO3 Oxidation Products from the
827 RO2 + HO2 Pathway, The Journal of Physical Chemistry A, 10.1021/acs.jpca.5b06355, 2015.

828 Shao, Y., Gan, Z., Epifanovsky, E., Gilbert, A. T. B., Wormit, M., Kussmann, J., Lange, A. W., Behn,
829 A., Deng, J., Feng, X., Ghosh, D., Goldey, M., Horn, P. R., Jacobson, L. D., Kaliman, I., Khaliullin, R.
830 Z., Kuś, T., Landau, A., Liu, J., Proynov, E. I., Rhee, Y. M., Richard, R. M., Rohrdanz, M. A., Steele,
831 R. P., Sundstrom, E. J., Woodcock, H. L., Zimmerman, P. M., Zuev, D., Albrecht, B., Alguire, E.,
832 Austin, B., Beran, G. J. O., Bernard, Y. A., Berquist, E., Brandhorst, K., Bravaya, K. B., Brown, S. T.,
833 Casanova, D., Chang, C.-M., Chen, Y., Chien, S. H., Closser, K. D., Crittenden, D. L., Diedenhofen,
834 M., DiStasio, R. A., Do, H., Dutoi, A. D., Edgar, R. G., Fatehi, S., Fusti-Molnar, L., Ghysels, A.,
835 Golubeva-Zadorozhnaya, A., Gomes, J., Hanson-Heine, M. W. D., Harbach, P. H. P., Hauser, A. W.,
836 Hohenstein, E. G., Holden, Z. C., Jagau, T.-C., Ji, H., Kaduk, B., Khistyaev, K., Kim, J., Kim, J., King,
837 R. A., Klunzinger, P., Kosenkov, D., Kowalczyk, T., Krauter, C. M., Lao, K. U., Laurent, A. D., Lawler,
838 K. V., Levchenko, S. V., Lin, C. Y., Liu, F., Livshits, E., Lochan, R. C., Luenser, A., Manohar, P., Manzer,
839 S. F., Mao, S.-P., Mardirossian, N., Marenich, A. V., Maurer, S. A., Mayhall, N. J., Neuscamman, E.,
840 Oana, C. M., Olivares-Amaya, R., O'Neill, D. P., Parkhill, J. A., Perrine, T. M., Peverati, R., Prociuk,
841 A., Rehn, D. R., Rosta, E., Russ, N. J., Sharada, S. M., Sharma, S., Small, D. W., Sodt, A., Stein, T.,
842 Stück, D., Su, Y.-C., Thom, A. J. W., Tsuchimochi, T., Vanovschi, V., Vogt, L., Vydrov, O., Wang, T.,
843 Watson, M. A., Wenzel, J., White, A., Williams, C. F., Yang, J., Yeganeh, S., Yost, S. R., You, Z.-Q.,
844 Zhang, I. Y., Zhang, X., Zhao, Y., Brooks, B. R., Chan, G. K. L., Chipman, D. M., Cramer, C. J., Goddard,
845 W. A., Gordon, M. S., Hehre, W. J., Klamt, A., Schaefer, H. F., Schmidt, M. W., Sherrill, C. D., Truhlar,
846 D. G., Warshel, A., Xu, X., Aspuru-Guzik, A., Baer, R., Bell, A. T., Besley, N. A., Chai, J.-D., Dreuw,
847 A., Dunietz, B. D., Furlani, T. R., Gwaltney, S. R., Hsu, C.-P., Jung, Y., Kong, J., Lambrecht, D. S.,
848 Liang, W., Ochsenfeld, C., Rassolov, V. A., Slipchenko, L. V., Subotnik, J. E., Van Voorhis, T., Herbert,
849 J. M., Krylov, A. I., Gill, P. M. W., and Head-Gordon, M.: Advances in molecular quantum chemistry
850 contained in the Q-Chem 4 program package, Molecular Physics, 113, 184-215,
851 10.1080/00268976.2014.952696, 2015.

852 Shepson, P. B., and Heicklen, J.: The wavelength and pressure dependence of the photolysis of
853 propionaldehyde in air, Journal of Photochemistry, 19, 215-227, http://dx.doi.org/10.1016/0047-
854 2670(82)80024-5, 1982.

855 Shepson, P. B., Bottenheim, J. W., Hastie, D. R., and Venkatram, A.: Determination of the relative
856 ozone and PAN deposition velocities at night, Geophysical Research Letters, 19, 1121-1124,
857 10.1029/92GL01118, 1992.

Sprengnether, M., Demerjian, K. L., Donahue, N. M., and Anderson, J. G.: Product analysis of the OH oxidation of isoprene and 1,3-butadiene in the presence of NO, Journal of Geophysical Research, 107, 10.1029/2001jd000716, 2002.

Starn, T. K., Shepson, P. B., Bertman, S. B., Riemer, D. D., Zika, R. G., and Olszyna, K.: Nighttime isoprene chemistry at an urban-impacted forest site, Journal of Geophysical Research: Atmospheres, 103, 22437-22447, 10.1029/98JD01201, 1998.

Su, L., Patton, E. G., Vilà-Guerau de Arellano, J., Guenther, A. B., Kaser, L., Yuan, B., Xiong, F., Shepson, P. B., Zhang, L., Miller, D. O., Brune, W. H., Baumann, K., Edgerton, E., Weinheimer, A., and Mak, J. E.: Understanding isoprene photo-oxidation using observations and modelling over a subtropical forest in the Southeast US, Atmos. Chem. Phys. Discuss., 15, 31621-31663, 10.5194/acpd-15-31621-2015, 2015.

Suarez-Bertoa, R., Picquet-Varrault, B., Tamas, W., Pangui, E., and Doussin, J. F.: Atmospheric fate of a series of carbonyl nitrates: photolysis frequencies and OH-oxidation rate constants, Environmental science & technology, 46, 12502-12509, 10.1021/es302613x, 2012.

Treacy, J., Hag, M. E., O'Farrell, D., and Sidebottom, H.: Reactions of Ozone with Unsaturated Organic Compounds, Berichte der Bunsengesellschaft für physikalische Chemie, 96, 422-427, 10.1002/bbpc.19920960337, 1992.

Tuazon, E. C., Atkinson, R., Mac Leod, H., Biermann, H. W., Winer, A. M., Carter, W. P. L., and Pitts, J. N.: Yields of glyoxal and methylglyoxal from the nitrogen oxide(NOx)-air photooxidations of toluene and m- and p-xylene, Environmental science & technology, 18, 981-984, 10.1021/es00130a017, 1984.

Tuazon, E. C., and Atkinson, R.: A product study of the gas-phase reaction of Isoprene with the OH radical in the presence of NOx, International Journal of Chemical Kinetics, 22, 1221-1236, 10.1002/kin.550221202, 1990.

Vingarzan, R.: A review of surface ozone background levels and trends, Atmospheric Environment, 38, 3431-3442, http://dx.doi.org/10.1016/j.atmosenv.2004.03.030, 2004.

Wang, X., Wang, T., Yan, C., Tham, Y. J., Xue, L., Xu, Z., and Zha, Q.: Large daytime signals of N2O5 and NO3 inferred at 62 amu in a TD-CIMS: chemical interference or a real atmospheric phenomenon?, Atmos. Meas. Tech., 7, 1-12, 10.5194/amt-7-1-2014, 2014.

Wiberg, K. B., Hadad, C. M., Rablen, P. R., and Cioslowski, J.: Substituent effects. 4. Nature of substituent effects at carbonyl groups, Journal of the American Chemical Society, 114, 8644-8654, 10.1021/ja00048a044, 1992.

Wu, S., Mickley, L. J., Jacob, D. J., Logan, J. A., Yantosca, R. M., and Rind, D.: Why are there large differences between models in global budgets of tropospheric ozone?, Journal of Geophysical Research: Atmospheres, 112, D05302, 10.1029/2006JD007801, 2007.

Xie, Y., Paulot, F., Carter, W. P. L., Nolte, C. G., Luecken, D. J., Hutzell, W. T., Wennberg, P. O., Cohen, R. C., and Pinder, R. W.: Understanding the impact of recent advances in isoprene photooxidation on simulations of regional air quality, Atmospheric Chemistry and Physics, 13, 8439-8455, 10.5194/acp-13-8439-2013, 2013.

Xiong, F., McAvey, K. M., Pratt, K. A., Groff, C. J., Hostetler, M. A., Lipton, M. A., Starn, T. K., Seeley, J. V., Bertman, S. B., Teng, A. P., Crounse, J. D., Nguyen, T. B., Wennberg, P. O., Misztal, P. K., Goldstein, A. H., Guenther, A. B., Koss, A. R., Olson, K. F., de Gouw, J. A., Baumann, K., Edgerton, E. S., Feiner, P. A., Zhang, L., Miller, D. O., Brune, W. H., and Shepson, P. B.: Observation of isoprene hydroxynitrates in the southeastern United States and implications for the fate of NOx, Atmos. Chem. Phys., 15, 11257-11272, 10.5194/acp-15-11257-2015, 2015.

Zellner, R., and Lorenz, K.: Laser photolysis/resonance fluorescence study of the rate constants for the reactions of hydroxyl radicals with ethene and propene, The Journal of Physical Chemistry, 88, 984-989, 10.1021/j150649a028, 1984.

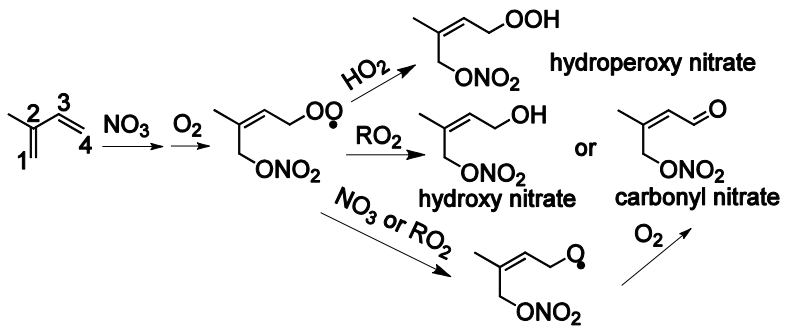

Figure 1. Organic nitrates produced from NO_3-initiated isoprene oxidation.

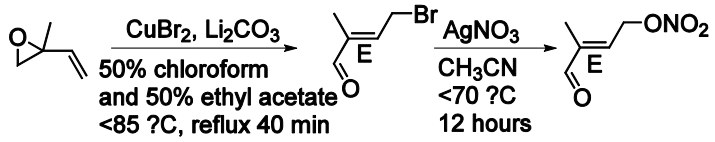

Figure 2. The synthesis route for the 4,1-isoprene ~~carbonyl nitrate~~nitrooxy enal.

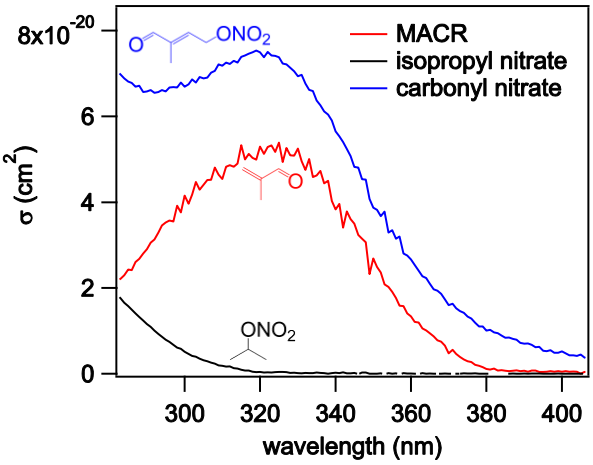

Figure 3. UV absorption cross section of the ~~carbonyl nitrate~~nitrooxy enal, MACR and isoproyl nitrate. The spectra were all obtained in acetonitrile solvent.

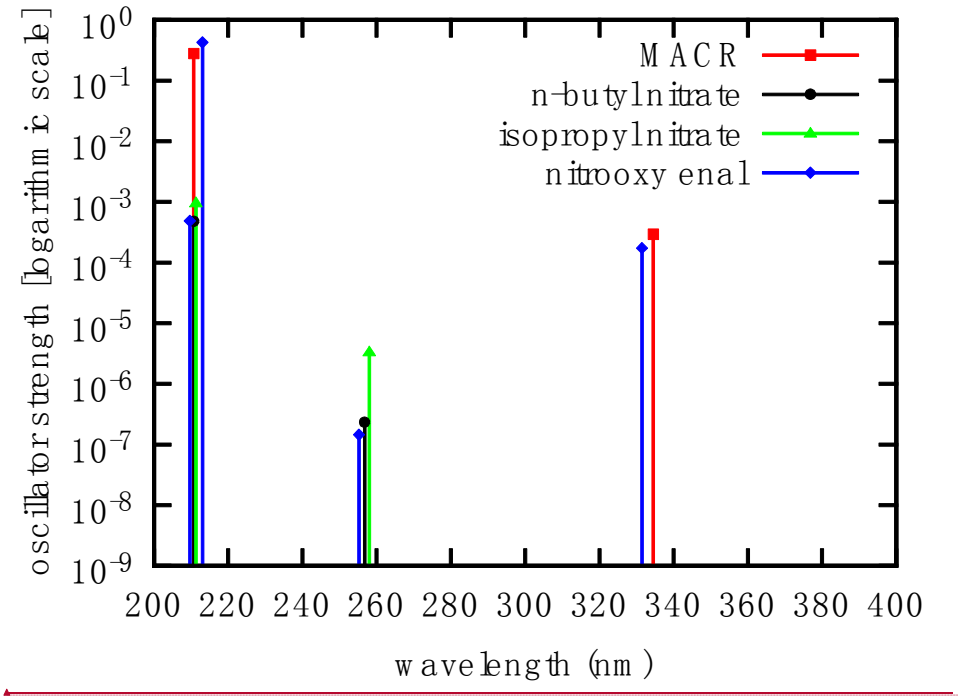

Figure 4. Theoretical gas-phase absorption spectra of the ~~carbonyl nitrate~~nitrooxy enal, MACR, isopropyl nitrate and *n*-butyl nitrate in the gas phase.

Formatted: Font: (Default) Arial

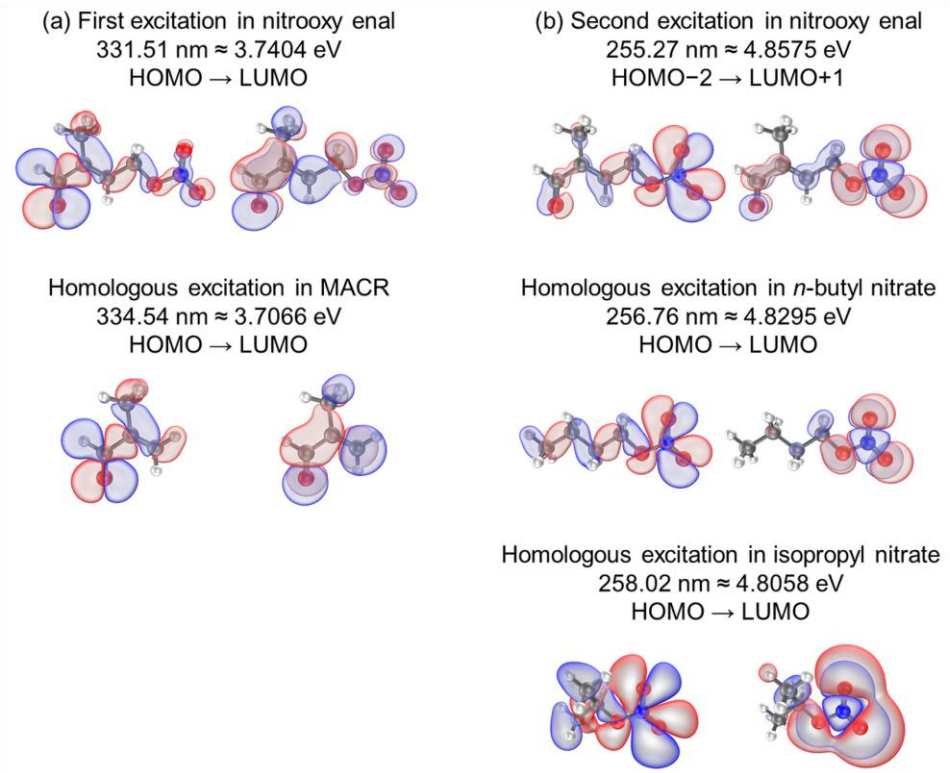

Figure 5. Molecular orbital analysis of the first (a) and second (b) electronic excitations of the ~~carbonyl nitrate~~nitrooxy enal, along with analogous excitations of MACR, isopropyl nitrate and n-butyl nitrate. The blue and red colors represent the opposite phases of molecular orbitals.

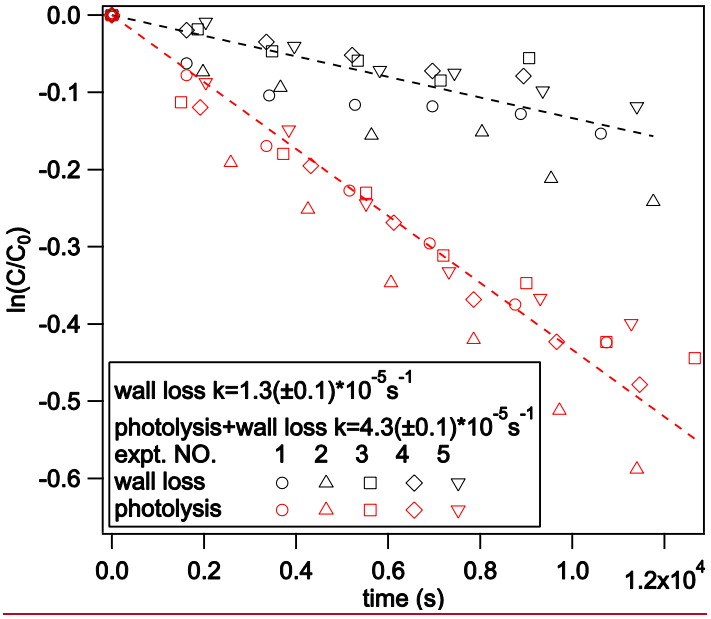

Figure 6. Wall loss and photolysis loss of the ~~carbonly nitrate~~nitrooxy enal in the reaction chamber.

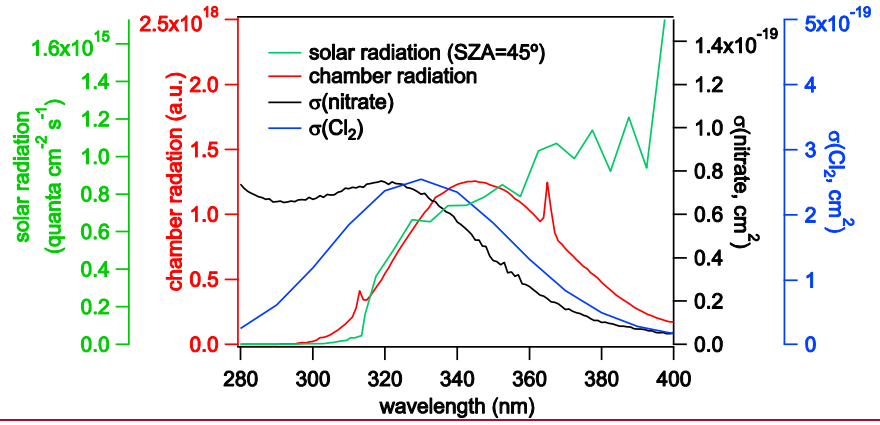

Figure 7. The radiation spectra of the chamber (red) and the sun (green, SZA=45° as an example), and the absorption spectra of the ~~carbonyl nitrate~~nitrooxy enal (black, obtained in the liquid phase using acetonitrile solvent) and chlorine (blue).

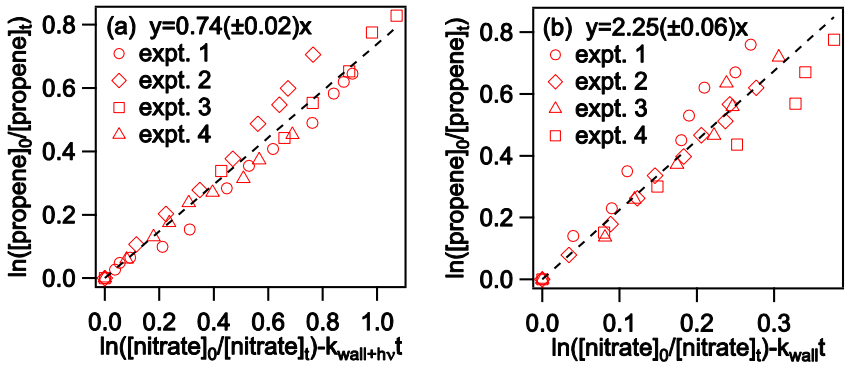

Figure 8. The first-order loss of propene relative to that of the ~~carbonyl nitrate~~nitrooxy enal for OH-initiated (a) and O_3-initiated (b) oxidation reactions.

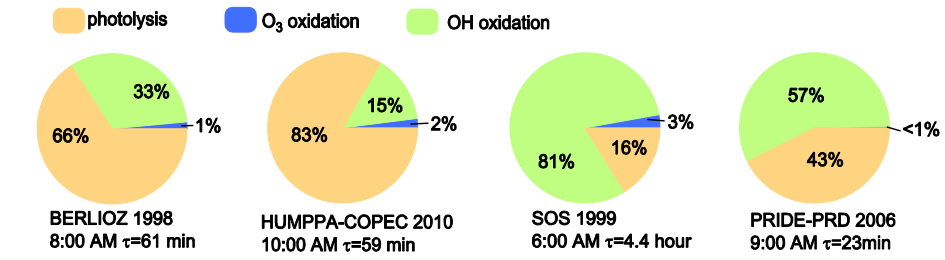

Figure 9. The relative contributions of photolysis (orange), OH oxidation (green) and O_3 oxidation (blue) to the photochemical decay of the ~~carbonyl nitrate~~nitrooxy enal, calculated based on measured OH and O_3 concentrations for the following field studies: BERLIOZ 1998 study at Pabstthum, Germany (Mihelcic et al., 2003; Platt et al., 2002), HUMPPA-COPEC 2010 study at Hyytiälä (Hens et al., 2014), Finland, SOS 1999 study at Nashville, US (Martinez et al., 2003; Roberts et al., 2002) and PRIDE-PRD 2006 study at Guangzhou, China (Lu et al., 2012).

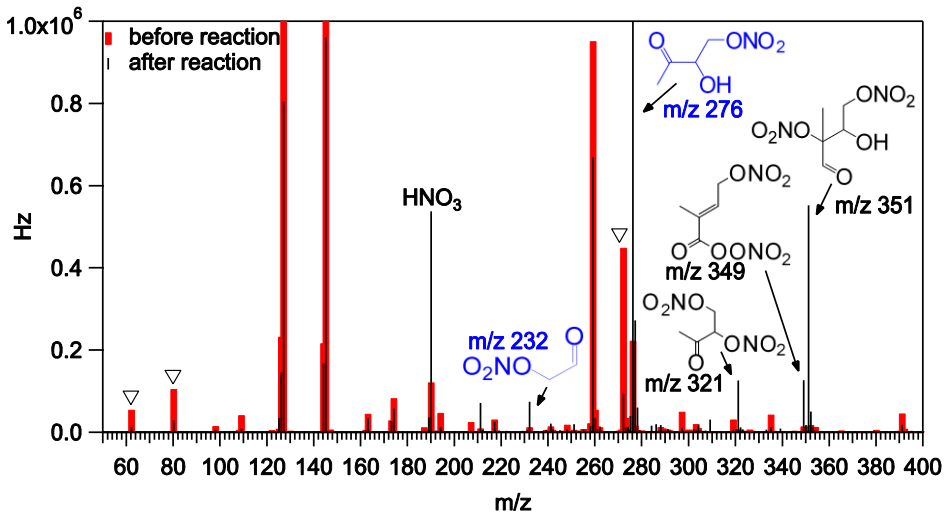

Figure 10. The CIMS spectra before (red) and after (black) the OH + ~~carbonyl nitrate~~nitrooxy enal oxidation reaction. The inverted triangles show the decreases in CIMS signals for the ~~carbonyl nitrate~~nitrooxy enal (m/z 272) and the NO_3^- fragments (m/z 62, water cluster at m/z 80) derived from the carbonyl nitrate (Fig. 11). The molecular structures are inferred from the nominal masses observed by CIMS. The compounds that were observed by both CIMS and GC (Fig. 13) are colored in blue.

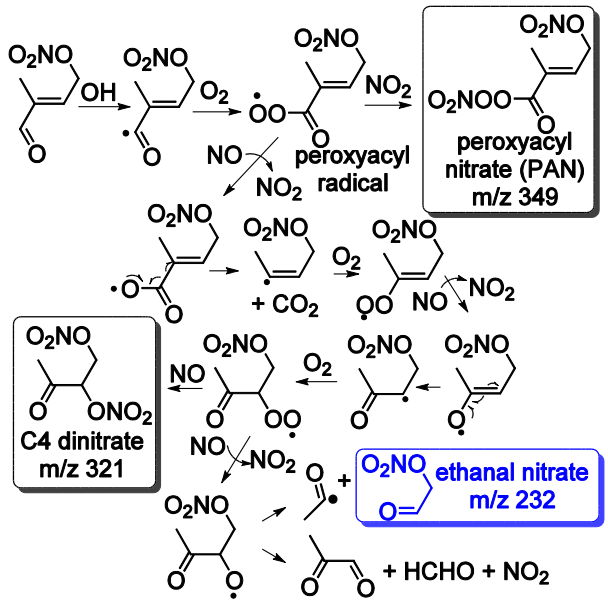

Figure 11. A proposed reaction mechanism for the H abstraction pathway for the OH + ~~carbonyl nitrate~~nitrooxy enal oxidation reaction. The compounds in boxes are ~~proposed~~ products inferred from ~~as~~the nominal masses observed by the CIMS (Fig. 8). The compound colored in blue was observed by both GC and CIMS (Fig. 13).

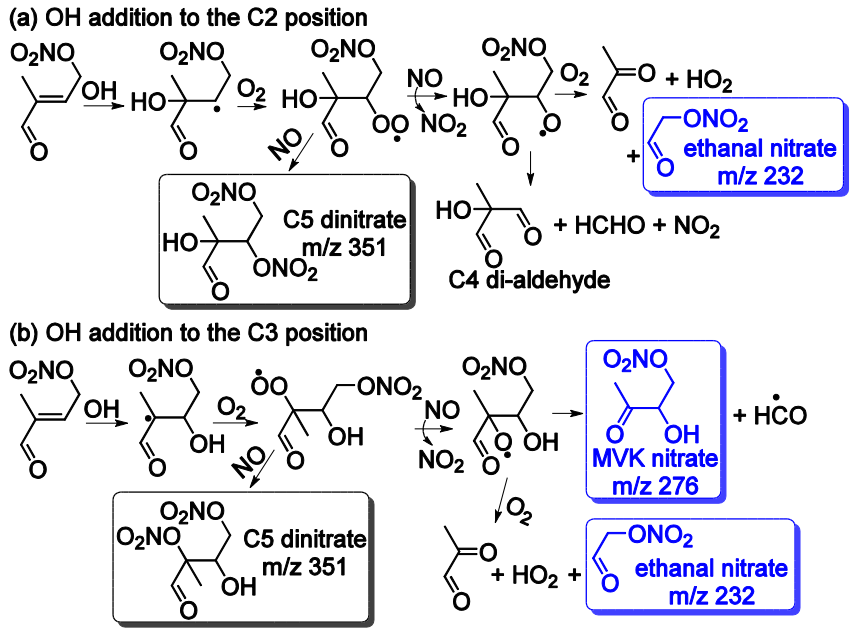

Figure 12. Proposed reaction mechanisms for OH addition to the C2 (a) and C3 (b) position of the ~~carbonyl nitrate~~nitrooxy enal. The compounds in boxes are ~~proposed~~ products inferred from the nominal masses~~as~~ observed by the CIMS (Fig. 8). The compounds that were observed by both CIMS and GC (Fig. 13) are colored in blue.

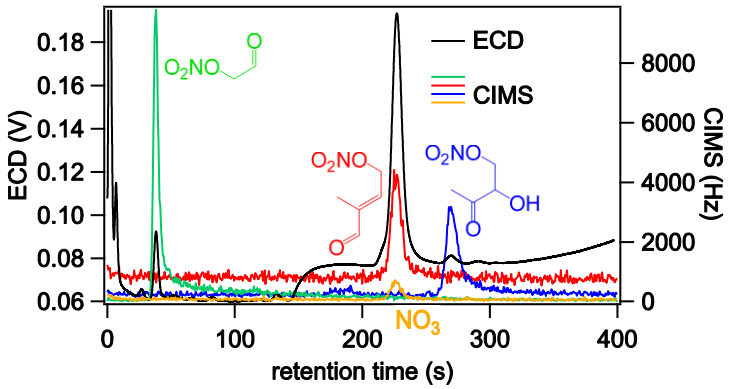

Figure 13. The GC-ECD/CIMS spectra for the ~~carbonyl nitrate~~nitrooxy enal (red), MVK nitrate (blue) and ethanal nitrate (green). The reaction of iodide with the ~~carbonyl nitrate~~nitrooxy enal generated NO_3^- ion (orange). The ECD chromatogram is shown in black.

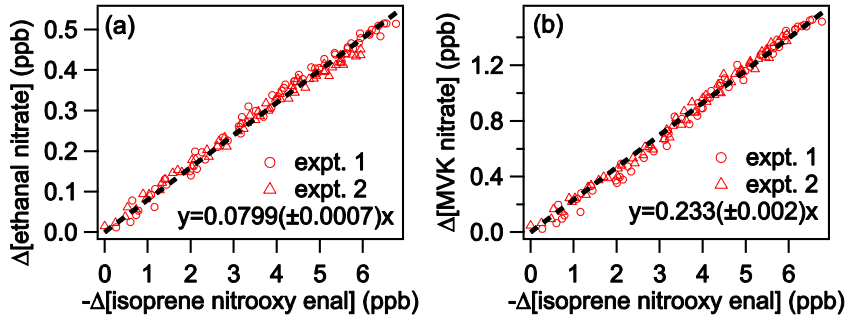

Figure 14. The formation of ethanal nitrate (a) and MVK nitrate (b) relative to the loss of the isoprene ~~carbonyl nitrate~~nitrooxy enal for the OH + ~~carbonyl nitrate~~nitrooxy enal oxidation experiments.

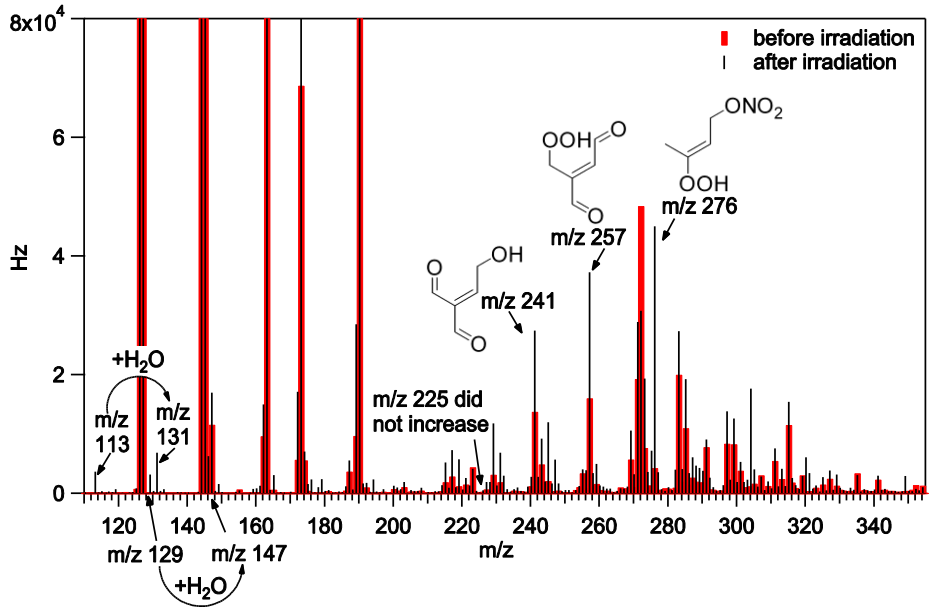

Figure 15. CIMS spectra before (red) and after (black) the photolysis of the isoprene ~~carbonyl nitrate~~nitrooxy enal. The molecular structures are inferred from the nominal masses observed by CIMS.

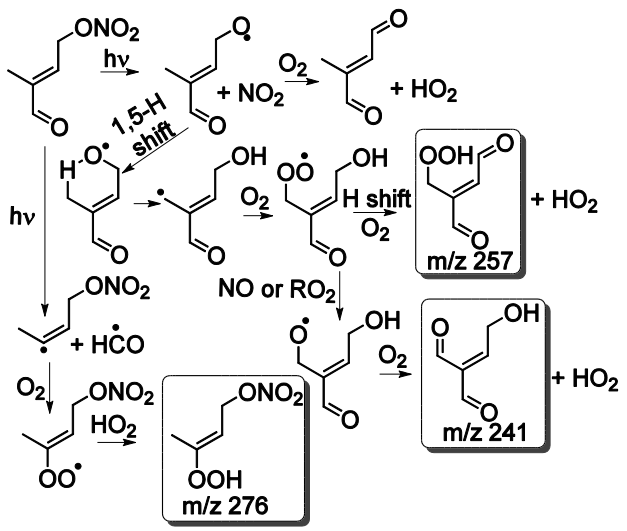

Figure 16. A proposed reaction mechanisms for the ~~carbonyl nitrate~~nitrooxy enal photolysis reaction. The compounds in boxes are ~~proposed~~ products ~~as~~inffered from nominal masses observed by the CIMS (Fig. 13).